



Contents lists available at ScienceDirect

Earth-Science Reviews

journal homepage: www.elsevier.com/locate/earscirev

Constraints to the timing of India–Eurasia collision; a re-evaluation of evidence from the Indus Basin sedimentary rocks of the Indus–Tsangpo Suture Zone, Ladakh, India

Alexandra L. Henderson ^a, Yani Najman ^{a,*}, Randall Parrish ^b, Darren F. Mark ^c, Gavin L. Foster ^d

^a Lancaster Environment Centre, Lancaster University, Lancashire, LA1 3YQ, UK

^b NERC Isotope Geosciences Laboratory, Kingsley Dunham Centre, Keyworth, Nottingham, NG12 5GG, UK

^c SUERC, Scottish Enterprise Technology Park, Rankine Avenue, East Kilbride, Glasgow, G75 0QF, UK

^d National Oceanography Centre Southampton, University of Southampton Waterfront Campus, European Way, Southampton, SO14 3ZH, UK

ARTICLE INFO

Article history:

Received 4 March 2010

Accepted 16 February 2011

Available online xxxx

Keywords:

Himalaya

India–Asia collision

Indus–Tsangpo suture zone

Indus molasse

ABSTRACT

Deposited within the Indus–Tsangpo suture zone, the Cenozoic Indus Basin sedimentary rocks have been interpreted to hold evidence that may constrain the timing of India–Eurasia collision, a conclusion challenged by data presented here. The Eurasian derived 50.8–51 Ma Chogdo Formation was previously considered to overlie Indian Plate marine sedimentary rocks in sedimentary contact, thus constraining the timing of collision as having occurred by this time. Using isotopic analysis (U–Pb dating on detrital zircons, Ar–Ar dating on detrital white mica, Sm–Nd analyses on detrital apatite), sandstone and conglomerate petrography, mudstone geochemistry, facies analysis and geological mapping to characterize and correlate the formations of the Indus Basin Sedimentary rocks, we review the nature of these contacts and the identification and correlation of the formations. Our results reveal that previously interpreted stratigraphic contacts identifying Chogdo Formation unconformably overlying Indian plate sedimentary rocks are incorrect. Rather, we suggest that the inaccuracy of previous interpretations is most likely a result of Formation misidentification and thus cannot be used to constrain the timing of India–Asia collision.

© 2011 Elsevier B.V. All rights reserved.

Contents

1.	Introduction	0
2.	Regional geology	0
3.	The Indus Basin sedimentary rocks: previous and current work	0
4.	Field area 1: The Lato–Upshi section	0
4.1.	Stratigraphy and structure	0
4.1.1.	The Miru Formation	0
4.1.2.	Gonmaru La Formation	0
4.1.3.	Artsa Formation	0
4.1.4.	Umlung Formation	0
4.1.5.	Upshi Formation	0
4.1.6.	Rong Formation	0
4.1.7.	Lato Formation	0
4.2.	Geochemical characteristics of the Formations.	0
4.2.1.	Mudstone geochemistry	0
4.2.2.	Sandstone petrography	0
4.2.3.	Conglomerate clast counts.	0
4.2.4.	²⁰⁶ Pb/ ²³⁸ U dating of detrital zircons	0
4.2.5.	⁴⁰ Ar/ ³⁹ Ar dating of detrital white micas	0
4.2.6.	Sm–Nd of detrital apatites.	0

* Corresponding author. Tel.: +44 1524 593898, +64 (0)21 261 9573 (currently).

E-mail address: y.najman@lancs.ac.uk (Y. Najman).

4.3.	Detrital provenance	0
4.3.1.	Provenance of the Indus Basin sedimentary rock formations	0
4.3.2.	Provenance of the Lato Formation	0
4.4.	IBSR stratigraphic correlation	0
4.4.1.	Correlation of the Miru Formation with the Tar Group in the Zaskar Gorge	0
4.4.2.	Correlation of the Gonmaru La, Artsa, Umlung, Upshi and Rong Formations with Indus Group rocks of the Zaskar Gorge	0
4.5.	Examining evidence for India–Eurasia collision from the Upshi–Lato section (Table 2)	0
4.6.	Suggested paleodepositional environment reconstruction for the IBSR.	0
5.	Field area 2: The Chilling–Sumda section, Zaskar Gorge	0
5.1.	Stratigraphy and structure	0
5.1.1.	Jurutze Formation	0
5.1.2.	Lower Chilling Formation	0
5.1.3.	Upper Chilling Formation	0
5.1.4.	Chilling ophiolitic mélange.	0
5.2.	Compositional characterization of the Chilling Formation.	0
5.2.1.	Mudstone geochemistry	0
5.2.2.	Sandstone petrography	0
5.2.3.	Conglomerate clast counts	0
5.2.4.	U–Pb ages of detrital zircons	0
5.3.	Provenance of the Chilling Formation	0
5.4.	Correlation of the Chilling Formation	0
5.5.	Examining evidence for India–Eurasia collision at the Chilling–Sumda section	0
6.	Summary and conclusions.	0
	Acknowledgements	0
	References	0

1. Introduction

It has been widely demonstrated that the evolution of the Himalaya has influenced many external factors including oceanic geochemistry (e.g. Richter et al., 1992), atmospheric circulation and global climate during the Cenozoic (e.g. Raymo and Ruddiman, 1992). In order to assess the extent to which these have been caused by mountain building processes it is necessary to understand Himalayan orogenic events, in particular the timing of India–Eurasia continental collision. However, despite the importance for constraining the timing of collision, the date of initial collision is still disputed; the general consensus places it around 50–55 Ma (e.g. Powell and Conaghan, 1973; Tonarini et al., 1993; de Sigoyer et al., 2000; Clift et al., 2002; Leech et al., 2005), with more extreme estimations ranging from 34 Ma to ~70 Ma (e.g. Ding et al., 2005; Yin, 2006; Aitchison et al., 2007). Part of this discrepancy is due to different definitions of collision and the variety of approaches to measuring it (e.g. Rowley, 1996). Examples of current methods used for constraining the timing of collision include dating of the ultra-high pressure eclogites which represent continental subduction (Tonarini et al., 1993; Leech et al., 2005; Parrish et al., 2006), earliest evidence of similar terrestrial faunas found on both Indian and Eurasian plates (Jaeger et al., 1989; Rage et al., 1995), and the time of deceleration of Indian Plate velocity (Molnar and Tapponnier, 1975; Patriat and Achache, 1984; Klootwijk et al., 1992).

Continental collisions bring about marked changes in sedimentation patterns in adjacent basins due to loading and subsidence, sedimentation rates, and/or a change in nature of sedimentation (e.g. a new detrital provenance; Rowley, 1996), thus making the sedimentary record of collision a useful tool to constrain the timing of collision and a means to improve understanding of early orogenic events. It is for these reasons that a range of extensive studies across the Himalayan range have been conducted, primarily focusing on Cenozoic aged sedimentary sequences which span the proposed age of collision.

This study focuses on the Indus Basin sedimentary rocks (IBSR; Fig. 1); a Cenozoic aged sequence of carbonate and clastic sediments deposited within the Indus Tsangpo Suture Zone (which separates the Indian and Eurasian plates) in northern India during the early phases

of India–Eurasia collision. The nature of the IBSR has been examined by several authors; (e.g. van Haver, 1984; Garzanti et al., 1987; Searle et al., 1990; Sinclair and Jaffey, 2001; Clift et al., 2002; Henderson et al., 2010b); with all work agreeing that sediments were dominantly sourced from the Eurasian margin, and deposited south of the Kohistan Ladakh Batholith between Early to ~Mid Cenozoic times, thus spanning the most commonly quoted age of collision of around 50–55 Ma. The stratigraphy appears to provide an excellent record of erosion that occurred during Indian–Eurasia collision. Previous studies of the IBSR constrained the time of India–Eurasia collision using the time of cessation of marine facies (Searle et al., 1990), first arrival of Eurasian detritus on the Indian plate (Clift et al., 2001, 2002) and/or earliest record of mixed Indian and Eurasian detritus in the sedimentary rocks (Clift et al., 2002; Wu et al., 2007; Henderson et al., 2010b). In this paper, we re-examine the evidence at key locations, and introduce new data from the IBSR to re-assess constraints to the timing of India–Eurasia collision. In contrast to previous work, we conclude that Eurasian derived sediments of 51 Ma do not stratigraphically overlie Indian plate rocks, and thus cannot be used to constrain the time of collision in the manner previously proposed.

2. Regional geology

As shown in Fig. 1, to the north of the Indus Tsangpo Suture Zone lie Eurasian Plate lithologies of the Lhasa–Karakoram Block and the Kohistan–Ladakh Island Arc. The Lhasa–Karakoram Block consists of Mid Proterozoic–Early Cambrian basement, overlain by low grade metamorphosed Palaeozoic to Mesozoic sedimentary rocks (Yin and Harrison, 2000; Henderson et al., 2010b). Both the Lhasa and Karakoram terranes are considered to have once existed as a single geological unit now separated by the Karakoram Fault (e.g. Searle et al., 1988). To the south of the Lhasa–Karakoram Block lies what was originally the Kohistan–Ladakh Island Arc, created by north directed intra-oceanic subduction within the Tethyan oceanic crust. Most recent papers consider that this arc collided with the southern Eurasian Margin prior to India–Asia collision, during mid to late Cretaceous times (e.g. Searle et al., 1988; Treloar et al., 1989, 1996; Sutra, 1990; Robertson and Degnan, 1994), although note new work

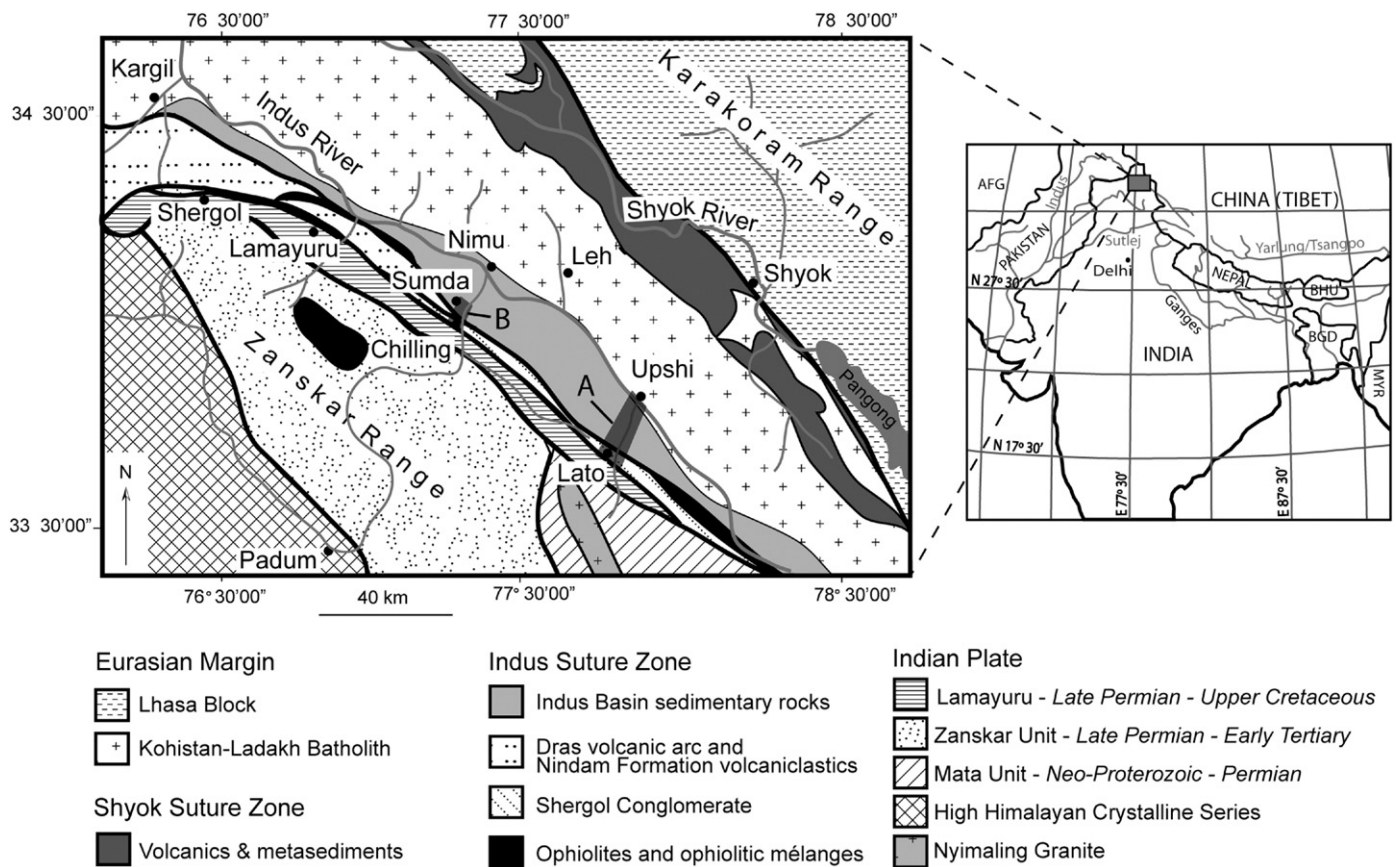


Fig. 1. Regional geology of Ladakh adapted from Mahéo et al. (2004), Robertson (2000), Honegger et al. (1989) and Steck (2003). Lato–Upshi study area (A) and Chilling–Sumda study area (B) are indicated by the gray boxes. Thick black lines depict faults, and rivers are represented by gray lines. AFG = Afghanistan, BHU = Bhutan, BGD = Bangladesh, MYR = Myanmar.

by Bouilhol et al., 2010, which suggests arc collision with India prior to Asia, the significance of which is discussed in Section 6. Marking the region of collision between the Lhasa–Karakoram Block and Kohistan–Ladakh Island Arc is the Shyok Suture Zone, composed mainly of ophiolitic mélangé and molasse. Subduction beneath Eurasia continued after arc–continent collision, forming the Trans-Himalayan batholith, referred to locally in the western Himalaya as the Ladakh Batholith, and overall consisting of Jurassic–Early Cenozoic calc-alkaline granitoids (Schärer et al., 1984), and associated Cenozoic volcanic sequences (e.g. the Linzizong Formation; Chung et al., 2005).

South of the Indus Tsangpo Suture Zone lie terrains of Indian Plate affinities. Directly south of the Indus Tsangpo Suture Zone is the carbonate and siliciclastic Tibetan Sedimentary Series, representing Paleozoic–Eocene deposition on the northern passive margin of India prior to India–Eurasia collision (Gaetani and Garzanti, 1991). Comprising part of the Tibetan Sedimentary Series exists the Lamayuru Formation representing Late Permian–Upper Cretaceous sedimentation on the Indian continental slope (Brookfield and Andrews-Speed, 1984; Robertson and Degnan, 1993; Robertson, 1998), and Permian–Eocene Indian continental shelf carbonates of the Zaskar Unit (Fuchs, 1981; Gaetani and Garzanti, 1991). Emplaced above the Zaskar Unit is the Spontang ophiolite and associated ophiolitic mélangé; however, the timing of this obduction is disputed with current estimates ranging from late Cretaceous (e.g. Searle et al., 1987, 1997; Corfield et al., 1999) to Eocene (e.g. Garzanti et al., 1987; Gaetani and Garzanti, 1991).

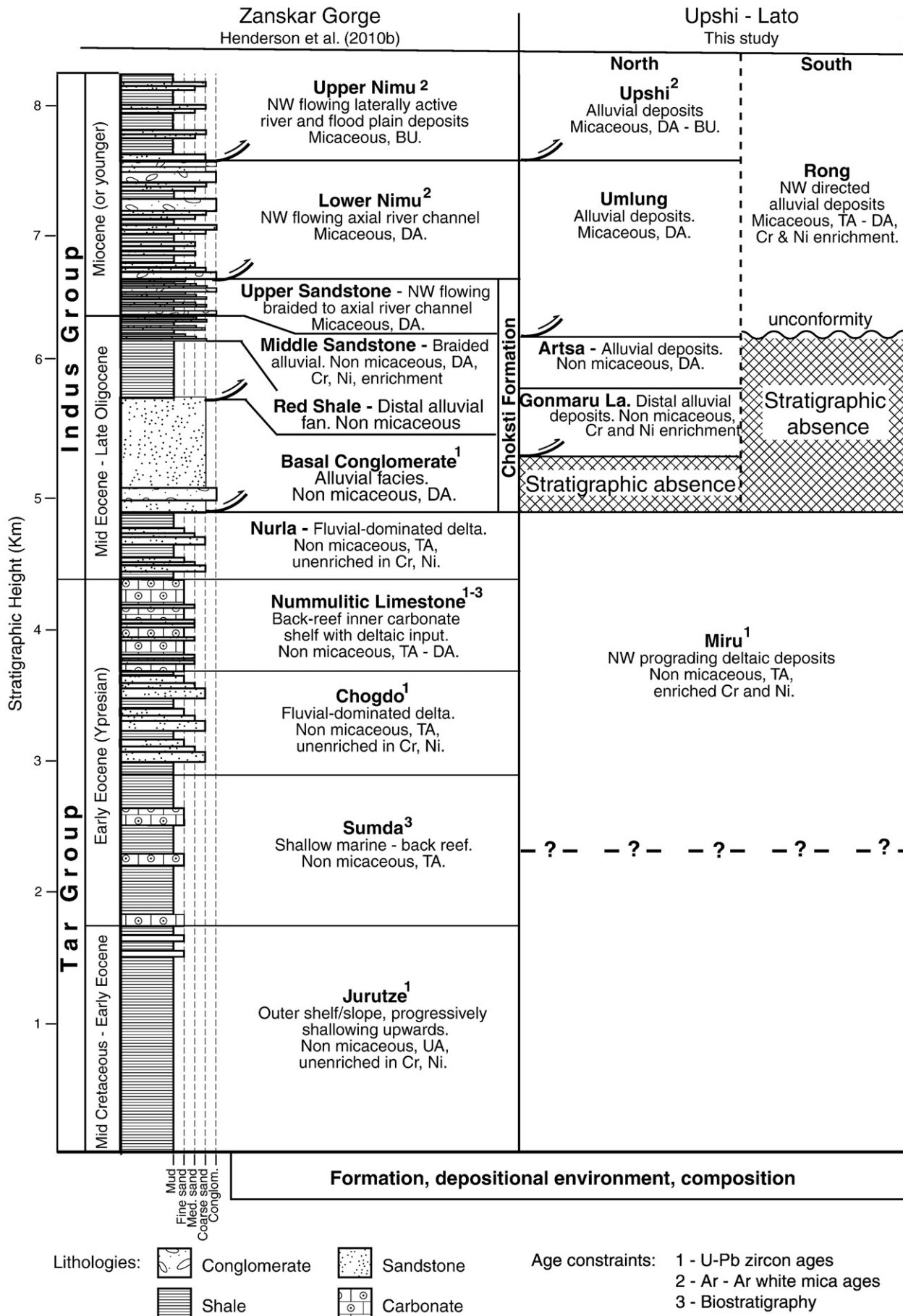
To the south of the Tibetan Sedimentary Series, separated by a large extensional fault system known as the South Tibet Detachment Zone, the rocks comprising the Higher Himalayan Crystalline Series have been subjected to different degrees of regional metamorphism developed during post-collisional times (Searle et al., 1992; Vannay

and Hodges, 1996; Vance and Harris, 1999; Walker et al., 1999; Foster et al., 2000; Simpson et al., 2000). The original Neoproterozoic protolith of the Higher Himalayan Crystalline Series is still preserved in places affected only by low grade metamorphic conditions and referred to as the Haimanta Formation (Miller et al., 2001). To the south of the Higher Himalayan Crystalline Series, separated by the Main Central Thrust lies the Lesser Himalaya, composed of low grade or unmetamorphosed Indian crustal rocks of dominantly Precambrian to Palaeozoic age (Valdiya and Bhatia, 1980; Tewari, 1993; Oliver et al., 1995).

The dominant units within the Indus Tsangpo Suture Zone (and also the focus of this study), consist of the Cenozoic IBSR; a sequence of marine and terrestrial facies consisting of detritus eroded from the Eurasian and Indian plates during collision, and described in detail below. Also within the Indus Tsangpo Suture Zone, occurring south of the IBSR in western Ladakh lie the Dras Arc units. These consist of basaltic pillow lavas representative of intraoceanic volcanism initiated during the Early Cretaceous, and associated forearc deposited volcanoclastic turbidite sediments of the Nindam Formation (Reuber, 1989; Sutra, 1990; Robertson and Degnan, 1994; Clift et al., 2000). Associated with the Nindam Formation are Aptian platform carbonates of the Khalsi Limestone. A series of ophiolitic mélanges also exist within the Indus Tsangpo Suture Zone, which have been divided into northern and southern zones in relation to the Dras Arc complex (Robertson, 2000).

3. The Indus Basin sedimentary rocks: previous and current work

The IBSR make up the dominant units within the Indus Tsangpo Suture Zone, recording the Paleogene marine to terrestrial sedimentary deposition which occurred in the suture zone during India–



Eurasia collision. The IBSR can be divided into two groups (Fig. 2). The older Tar Group (>49.4 Ma) consists of an upward-shallowing sequence from marine shales and shallow marine carbonates to fluvial dominated deltaic deposits (Searle et al., 1990; Sinclair and Jaffey, 2001; Henderson et al., 2010b), representing the demise of Neo-Tethys which early workers interpreted to be in a forearc setting (e.g. Garzanti and van Haver, 1988; Clift et al., 2002). However, more recent work suggests deposition occurred in an arc-bound basin setting between the Kohistan–Ladakh Island Arc to the north and the easterly discontinuous Dras Arc to the south (Henderson et al., 2010b). Sitting conformably above the Tar Group, the Indus Group (Baud et al., 1982; Garzanti and van Haver, 1988) represents terrestrial deposition and shows a progressive evolution from fluvial dominated deltaic facies in mid Eocene times, to alluvial facies and finally the development of a single channel NW-directed river system in Early Miocene times, considered by Henderson et al. (2010b) to represent the earliest paleo-Indus River deposits in this region.

A number of previous workers carried out initial stratigraphic work (e.g. Brookfield and Andrews-Speed, 1984; van Haver, 1984; Garzanti and van Haver, 1988; Searle et al., 1990; Sinclair and Jaffey, 2001; Clift et al., 2002) on which the later work of Henderson et al. (2010b) was built. Throughout this study we have chosen to refer to the stratigraphy defined by Henderson et al. (2010b) based on IBSR units exposed within the Zaskar Gorge. A schematic summary of this stratigraphy detailing depositional environments and age constraints is given in Fig. 2.

The termination of marine sedimentation within the Indus Basin, marked by the 49.4–50.8 Ma aged Nummulitic Limestone (Green et al., 2008; Henderson et al., 2010b), was designated by Searle et al. (1990) to represent the final closure of Neo-Tethys Ocean, thus providing a minimum age to collision. Using petrographic studies of the IBSR, Clift et al. (2002) proposed that the Chogdo Formation (situated directly below the Nummulitic Limestone; Fig. 2, and dated at 51–50.8 Ma by Henderson et al., 2010b) contains conglomerate clasts of both Indian plate (e.g. peridotite from the Spongtag ophiolite) and Eurasian plate (e.g. granitoid from the Trans-Himalaya) origin, allowing these authors to suggest that India–Eurasia collision had occurred before or during the deposition of the Chogdo Formation. However, Henderson et al. (2010b) considered that the presence of ophiolitic detritus did not constitute robust evidence of Indian plate input since such material could have been derived from local sources within the Indus Tsangpo Suture Zone related to the Dras Arc. Furthermore, a reassessment of the paleodepositional environments of the IBSR by Henderson et al. (2010b) suggested that the lower and middle stratigraphic levels of the IBSR, which includes the Chogdo Formation, were more likely deposited within an arc-bound basin between the Dras arc and Kohistan–Ladakh Island Arc, as opposed to the forearc basin environment of deposition suggested in some previous studies (e.g. Garzanti and van Haver, 1988; Clift et al., 2002). This “closed” arc-bound basin paleogeography renders the deliverance of Indian plate material into the basin less likely, particularly into the lower IBSR stratigraphic levels.

U–Pb detrital zircon dating (Wu et al., 2007; Henderson et al., 2010b) has shown that Jurassic to mid Eocene aged Eurasian derived grains form the dominant detrital zircon population throughout the IBSR. Hf isotopic characterization of IBSR detrital zircons was interpreted by Wu et al. (2007) to suggest that the subordinate number of Precambrian grains present in the older formations were also sourced from the Eurasian basement rather than India. The first unequivocal detrital evidence indicating an additional Indian plate

input to the IBSR, thus constraining the timing of collision, was recorded in the uppermost Choksti Formation (and subsequent younger stratigraphic levels), based on the presence of High Himalayan derived white micas (Henderson et al., 2010b). In addition, two detrital zircons; one with a Hf model age of 3.4 Ga and the other with a U–Pb age of 278 ± 2 Ma, are interpreted by Wu et al. (2007) as unique to Indian Plate terranes. Sm–Nd isotopic studies conducted by Henderson et al. (2010a) of in-situ detrital apatite grains from the IBSR failed to reveal any detrital apatite sourced from the Indian Plate; apatites were largely of Trans-Himalayan provenance with a possible additional Lhasa Block input at higher stratigraphic levels.

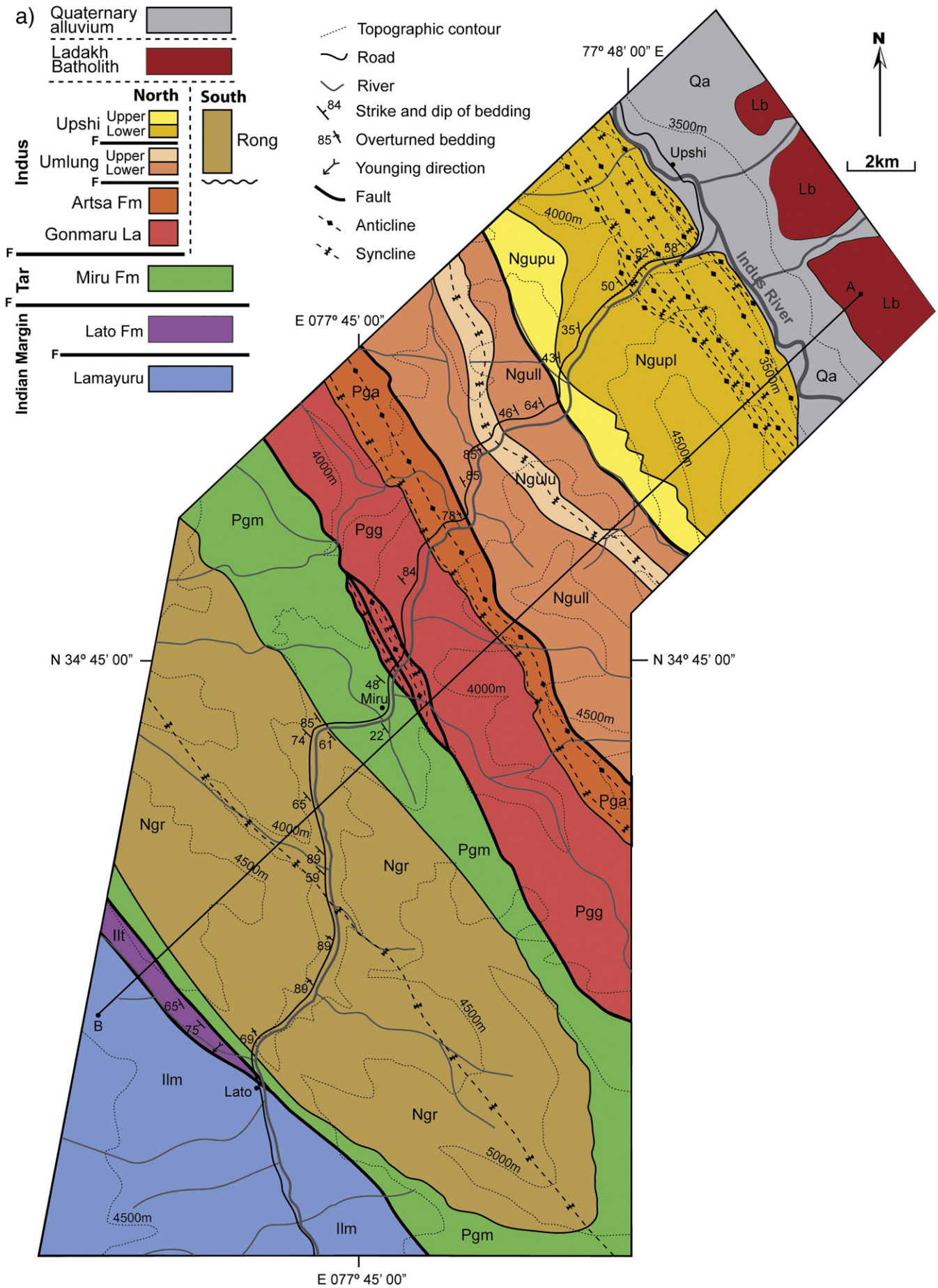
However, despite the lack of strong evidence of Indian-plate derived detritus occurring within the Lower IBSR, Clift et al. (2001, 2002) explored stratigraphic relationships within the IBSR to search for evidence of India–Eurasia collision. At two locations those authors identified red sedimentary rocks which they assigned to Eurasian derived Chogdo Formation, lying in angular erosional contact above shales they interpreted to be of the Indian Plate's Lamayuru Formation. This relationship was identified to occur near the village of Lato, (Fig. 1), and west of the village of Chilling (Fig. 1). The authors also identified at Chilling the Chogdo Formation unconformably overlying ophiolitic mélangé, which the authors considered to be equivalent to the Indian Plate related Southern mélangé zone of Robertson (2000). If correct, the presence of these contacts implies that deposition of the Eurasian derived Chogdo Formation between 51 and 50.8 Ma occurred directly onto Indian Plate lithologies, thus constraining collision to have occurred by this time.

The validity of these stratigraphic interpretations (and their importance for constraining the timing of collision) depends on a number of criteria: a) the certainty of the correct identity of the rocks lying below the unconformity (i.e. if they are of Indian origin as opposed to Eurasian origin), 2) the correct correlation of the sedimentary units sitting above the unconformity (i.e. if indeed the red sedimentary rocks belong to the Eurasian derived 50.8–51 Ma Chogdo Formation, as opposed to sediments of younger IBSR stratigraphy or of Indian origin), and 3) the true nature of the contact (i.e. stratigraphic as opposed to tectonic). To assess the validity of the correlations and contacts proposed by Clift et al. (2001, 2002) that are currently documented as showing evidence for India–Eurasia collision, we use a combination of field mapping, and petrographic, facies, isotopic, and geochemical analysis to explore the correlations and contacts in the two areas where Clift et al. (2001, 2002) observed the critical relationships: 1) between the villages of Upshi and Lato on the Manali–Leh Highway (Field area 1, Section 4) and 2) between Chilling and Sumda along the Zaskar Gorge (Field area 2, Section 5) (Fig. 1). Due to a combination of intense deformation, limited availability of biostratigraphic age constraints and lateral facies changes along strike, correlation and age constraints to the formations can be achieved best by a combination of geochemical, petrographic and isotopic characterization, comparing the units of interest to Tar and Indus Group characteristics from the “type-section” in the Zaskar Gorge, previously characterized by Henderson et al. (2010b).

4. Field area 1: The Lato–Upshi section

The geology exposed between the villages of Lato and Upshi on the Manali–Leh Highway, is the region where Clift et al. (2001, 2002) interpreted Eurasian derived IBSR Chogdo Formation to lie in unconformable contact above the Indian Plate derived Lamayuru Formation, thereby constraining collision to have occurred by 50.8 Ma

Fig. 2. Stratigraphic correlations between Indus Basin formations exposed along the Zaskar Gorge in the west (defined by Henderson et al., 2010b), and those identified further east outcropping along the Upshi–Lato transect from this study. Facies log represents IBSR lithologies in the Zaskar Gorge. Interpreted depositional environments are provided and compositional information is detailed when known. The following abbreviations refer to sandstone provenance fields as determined by Dickinson and Suczek (1979): BU = Basement Uplift, DA = Dissected Arc, TA = Transitional Arc, UA = Undissected Arc. Description of the methods used to determine age constraints are provided where applicable (nos. 1–3). The Lato Formation is not presented in this figure due to its current unknown stratigraphic relationship to the IBSR.



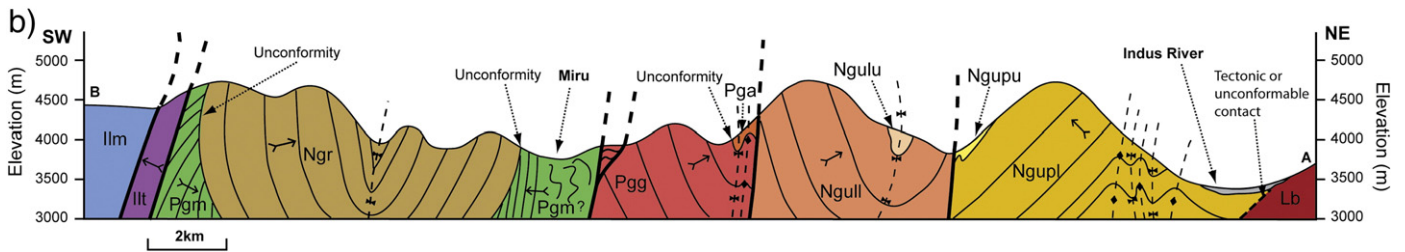


Fig. 3. a) Geological map constructed during field seasons in 2008–2009 between the villages of Upshi and Lato, Ladakh. Topographic contours are displayed in 500 m intervals taken from Pointet (2004). Stratigraphic key is constructed based on formations facies and composition (as discussed within Section 4), and faulted contacts are marked by “F”. b) Geological cross section between points A and B as displayed on the geological map in Fig. 3a. Approximate locations of villages are displayed, and younging directions are indicated. Key for Fig. 3: Pgm – Miru Fm; Pgg – Gonmaru La Fm; Pga – Artsa Fm; Ngull – Umlung Fm Lower; Ngulu Umlung Fm Upper; Ngupl – Upshi Fm Lower; Ngupu – Upshi Fm Upper; Ngr – Rong Fm; Ilt – Lato Fm; Ilm – Lamayuru Fm; Lb – Ladakh Batholith; Qa – Quaternary alluvium.

(maximum age of the Chogdo Formation dated in the Zaskar Gorge; Henderson et al., 2010b). To test whether the units are indeed Chogdo Formation and Lamayuru Formation as proposed, and whether the contact is unconformable as described, we present below the results of our work examining the facies, geochemical characteristics and provenance of the units exposed around this area and the nature of their contacts.

4.1. Stratigraphy and structure

In order to examine these proposed relationships we mapped a ~19 km section between the villages of Lato and Upshi (Figs. 1 and 3a and b). Facies and contacts mapped are summarized below, with more detailed sedimentology provided in Table 1. We present and define the geological formations based on the results of our mapping, petrographic, geochemical and isotopic characterization as described in Sections 4.1 and 4.2. In many cases, the formations which we identify are fault bound, making the construction of an accurate stratigraphy in the Lato–Upshi section challenging. Thus many of our IBSR correlations (presented in Section 4.5) and overall stratigraphic construction are based on similar isotopic, petrographic and/or lithological/facies characteristics shared between formations in the Lato–Upshi section of unknown stratigraphic height, correlated to those in the Zaskar Gorge with a known relative stratigraphic height (Fig. 2). The reasons as to why, in some cases, we do not agree with correlations of specific formations made in previous work, are discussed in Section 4.5.

4.1.1. The Miru Formation

The Miru Formation is folded into a NW–SE trending syncline, with its northern limb outcropping near the village of Miru, and its southern limb outcropping around the village of Lato, but here only for a limited section of stratigraphic exposure.

The Miru Formation's *northern limb* is well exposed around the village of Miru, consisting of blue-gray mudstones, light gray-black phyllitic shales and associated yellow-gray fine grained sandstones (Table 1, Fig. 4a and b). The sandstones particularly at the top of the Miru Formation contain an abundance of sedimentary structures (Fig. 5a and b) of which the structures most likely to be associated with the major flow (flute and gutter casts) give a northwest directed palaeoflow direction (Fig. 6). The southern extent of the exposure at the village of Miru is clearly visible showing coarse conglomeratic units of the Indus Group (Rong Formation; Section 4.1.6) unconformably overlying shales of the Miru Formation (Fig. 5c). The Rong Conglomerates are discontinuous and possess an erosional relationship down into the Miru Formation below. North of Miru village, the Miru Formation's northern contact is tectonically juxtaposed against a very deformed section of the Indus Group (Gonmaru La Formation; Section 4.1.2). This fault zone extends for ~150 m and contains

random blocks held within foreign lithologies and associated fault related fold deformation.

At the *southern limb*, near Lato, the Miru Formation consists dominantly of silver-gray-blue phyllites, red shales, and black-gray slates, with subordinate interbeds of fine-medium grained lithic arenites, small breccia beds and horizons and pebble conglomerates. The Miru Formation's southern contact at Lato is fault bound against the Lato Formation (see Section 4.1.7). Directly north of Lato, the Miru Formation is overlain by conglomerates of the Rong Formation, and it is here where Clift et al. (2001, 2002) assigned our defined Miru Formation, to the Indian Plate's Lamayuru Formation. We provide the reasons for our alternative correlation in Section 4.5, summarized in Table 2. An angular discordance in bedding is observed between the Miru and Rong Formations at this locality, implying the existence of an angular unconformity (Fig. 7); similar to what is observed just south of Miru on the northern limb of the syncline (Fig. 5c). Discontinuous sand lenses within the Miru Formation have rotated to align with the cleavage, most visible in the shales. The presence of slickensides and minor rotation of bedding in the Miru Formation directly beneath the Rong Formation implies that a degree of tectonization has also occurred along the contact.

4.1.2. Gonmaru La Formation

Structurally juxtaposed to the north of the Miru Formation's northern exposure exists a unit dominated by red shale (Fig. 4c, Table 1). This has been assigned to the Gonmaru La Formation by Garzanti and Van Haver (1988) and Fuchs and Linner (1996). It is characterized by red shales, which can vary to purple-brown in color. Red fine grained sandstone and purple medium grained sandstone beds also occur. Sedimentary structures are noted in Table 1 (see also Fig. 5d). The southern section of the unit, directly next to the faulted contact with the Miru Formation (Section 4.1.1) is deformed by a series of folds and faulting. Lithologies are generally coarser in this section with green coarse-medium lithic arenites alongside reddy-brown-purple fine sandstones, and red-blue-green shales. In agreement with Fuchs and Linner (1995), we identify the northern contact between the Gonmaru La and overlying Artsa Formations (Section 4.1.3) (Fig. 5e) to represent a conformable contact that has undergone a small degree of local shearing.

4.1.3. Artsa Formation

The Artsa Formation is composed of red shales, fine purple sandstones, gray-green coarse arkoses, and conglomerates (see Table 1 and Fig. 4d for detailed sedimentology). Northern (faulted) and southern (conformable) contacts are described in Sections 4.1.4 and 4.1.2, respectively.

4.1.4. Umlung Formation

Structurally bound to the north of the Artsa Formation, the Lower Umlung Formation consists of pebble conglomerates, coarse green

Table 1
Sedimentology of Formations described in Section 4, Field area 1, Lato–Upshi section, Manali–Leh Highway.

Lithologies and deformation	Sedimentology	Sedimentary structures	Suggested facies Interpretation
Miru Formation			
<i>Northern limb</i>			
Well-cleaved blue-green msts. Light-gray black phyllitic shales. Yellow gray fine-grained sst. Lignite and plant remains common. Intense deformation.	– Upward coarsening cycles sometimes present on 7–15 m scale, beginning with shales and subordinate sst, with increasing sst up-section.	Abundant, particularly in upper section: gutter and flute casts with associated current crescents and lunate ripples, symmetrical ripples, tool marks, x-lamination (often tabular), rip-up shales, load casts, burrows. Base of section: hummocky to swaley x-bedding.	Transition from shallow marine to prograding fluvial dominated delta, based on dominance of shales upward-coarsening to sst, common hummocky x-bedding and preservation of plant remains, gutter and flute casts at higher stratigraphic levels.
<i>Southern limb</i>			
Silver-gray-blue phyllites. Red well-cleaved shales. Black-gray slates. Fine-med grained lithic arenites. Small breccia beds/horizons. Pebble congl. Sst beds deformed and rotated to align with cleavage.	Dominantly fine-grained (shale) facies. Litharenites 1 cm–10 cm thick. Breccia beds: fine, angular to subangular autoclastic clasts and sand matrix. Conglomerates: clasts are exotic.		
Gonmaru La Formation			
Red to purple-brown well cleaved shales, red fine-grained ssts. Purple medium-grained ssts. Medium-coarse grained lithic arenites, red-purple-brown fine ssts and red-blue-green shales to south.	Shale dominated facies with 30–200 cm thick sst beds. Shale–sst alternations are rapid and irregular. Coarser to south.	Shales preserve dessication cracks and rarer raindrop imprints. Ssts preserve planar, wavy and ripple laminations, bifurcating lunate ripples and bioturbation. Shales associated with green reduction spots and horizons. In the south, rip-up shales and 30 cm trough x-beds also occur.	Alluvial facies, based on presence of pebble conglomerates, x-bedding, channelized bedding geometries, point bar deposits, and plant remains. Shale dominated facies indicative of overbank floodplain environment. Symmetrical ripples may indicate deposition in ephemeral lacustrine environments.
Artsa Formation			
Red shales, fine purple sands, gray-green coarse arkoses, and conglomerates.	Upward fining sequences on <1 m scale (Fig. 4d). Conglomerates are clast supported with coarse green litho-feldspathic matrix. Breccias and gritty laminations are common in the ssts, composed of autoclastic material.	Ssts have erosive bases and rip-up red shale clasts. Fine ssts have planar laminations and dewatering structures. Fine sands and shales have rare green reduction spots. Fine ssts and shales can display subtle intercalations.	
Umlung Formation			
Coarse green litharenites and arkoses, and finer green-red ssts. Red-purple-green cleaved shales. Subordinate conglomerates. Plant and wood remains. Black shales and sst present in upper section.	Congl, sst and shale arranged in upward fining sequences on 20–30 m scale, reduced to <10 m scale in upper parts. Conglomerate beds (<4–5 m thick and often laterally discontinuous over a >10 m scale) are clast supported by green sandy matrix.	Litharenites/ arkoses have erosive bases. Green reduction spots and horizons common in red shales. Black shale rip-up clasts, burrowing and dewatering structures, planar x-beds, sinuous-crested out-of-phase asymmetrical ripples and straight-crested to wavy symmetrical ripples.	
Upshi Formation			
<i>Lower part:</i> conglomerates, coarse green-red-blue-purple-gray sandstones and well-cleaved green and black shales. <i>Upper part:</i> fine-grained red-brown sst and red mst. Rare pebble congl.	<i>Lower part:</i> <50 m thick upward fining cycles. Congls are clast supported, and interbedded with 3–5 m long sst lenses. Ssts are lithic-rich with angular gritty texture. Ssts (<1 m thick) often have lenticular (channel) morphologies, discontinuous over 10 m. Ssts fine up into units dominated by green shales with interbeds of coarse green sst and black shale. <i>Upper part:</i> decreased grain-size, upward fining cycles on 40–150 m scale. Fine-grained red-brown sst and mst dominate, subordinate matrix-supported congl.	<i>Lower part:</i> Congls have erosive bases. Abundant cross and planar laminations, planar x-bedding, bioturbation in finer lithologies, and red rip-up shales in erosive-based units. <i>Upper part:</i> ssts have planar and x-lams depicted by distinct white and pink horizons. Msts and ssts have ripple lamination, load and flame structures and bioturbation.	
Rong Formation			
Coarse angular red-green litharenites. Fine-medium green or red sst. Conglomerates. Well cleaved red and blue shales	Upward fining sequences, on a scale of several decimeters, begins either with conglomerate or litharenite often with pebbly horizons or conglomeratic lenses (<1 m thick) and a channelized base. Fines up through medium-fine sst to shales. Shale dominated intervals of >20 m have 0.5 m thick fine red sst interbeds. Ssts can be of lenticular (channeled) morphology, >10 m width.	Ssts with erosive channeled base showing gutter casts and scour marks. Medium sst can have abundant planar cross-bedding. Fine sst can contain x-bedding, red shale rip-up clasts and green-white mottled reduction spots and horizons. Other structures include ripple x-beds and laminations, flute casts, wavy-straight crested symmetrical ripples, graded bedding, bioturbation. Massive x-bedded ssts (20–20 m scale, 5 m height) are interpreted as point bar deposits.	
Lato Fm			
Breccias, conglomerates, immature ssts and well cleaved blue & red shales & msts.	Overall upward-fining sequence.	Flaser bedding, ripple laminations, bioturbation, paleosols, load casts, dewatering structures, flute and gutter casts.	

sandstones and fine green-red sandstones, and red-purple-green shales (Fig. 4e, Table 1). Black shales and sandstones are present in the upper section. Sedimentary structures are common (as detailed in Table 1). Structurally the Umlung Formation is folded into a NW–SE trending synform, and is structurally bound to the north against the Upshi Formation (Fig. 5f).

4.1.5. Upshi Formation

The Upshi Formation is the most northerly occurring identified Indus Group formation in the Upshi–Lato section. A series of NW–SE trending folds have developed in the northern exposure of the formation, and folding has also developed in its southern extent where it is structurally bound with the Umlung Formation (Fig. 5f;

Section 4.1.4). Directly north of the mapped transect, the contact between the Upshi Formation and the Ladakh Batholith is obscured by scree.

Overall, the Upshi Formation youngs towards the SW. The Lower Upshi Formation consists of conglomerate, green-red-purple-blue-gray sandstone, and green and subordinately black shales (Table 1; Figs. 4f and 5f and g). Sedimentary structures are abundant, as documented in Table 1. Clast imbrication is apparent within the conglomerates. However, the presence of pebble pitting suggests that this should not be considered a reliable palaeoflow indicator as pebbles are likely to have rotated due to post-depositional deformation and thus their present day position is not guaranteed to represent their original depositional orientation.

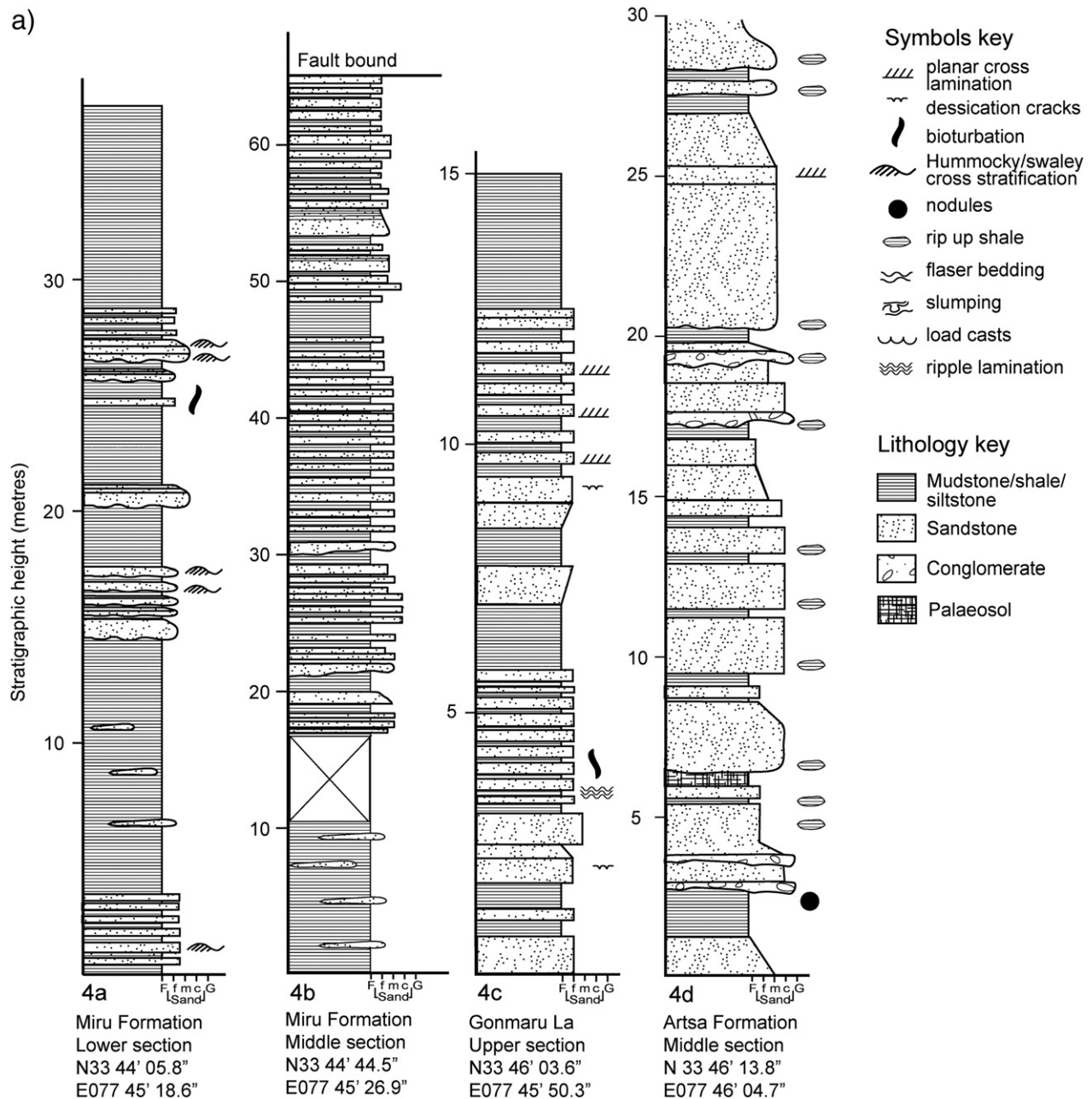


Fig. 4. a) Stratigraphic logs of select exposures of IBSR formations measured along the Upshi–Lato field area (4a–4h) as discussed in Section 4, and selected sections of the Lato Formation (4i) and Chilling Formation (4j–4k) as discussed in Sections 4 and 5. Stratigraphic level from where each measured section was taken, relative to each formation, is labeled. Grid reference localities indicate the position of the base of each log. F = Mud and fines, f = fine, m = medium, c = coarse, G = Gravel (conglomerate). Note that scales vary between each log.

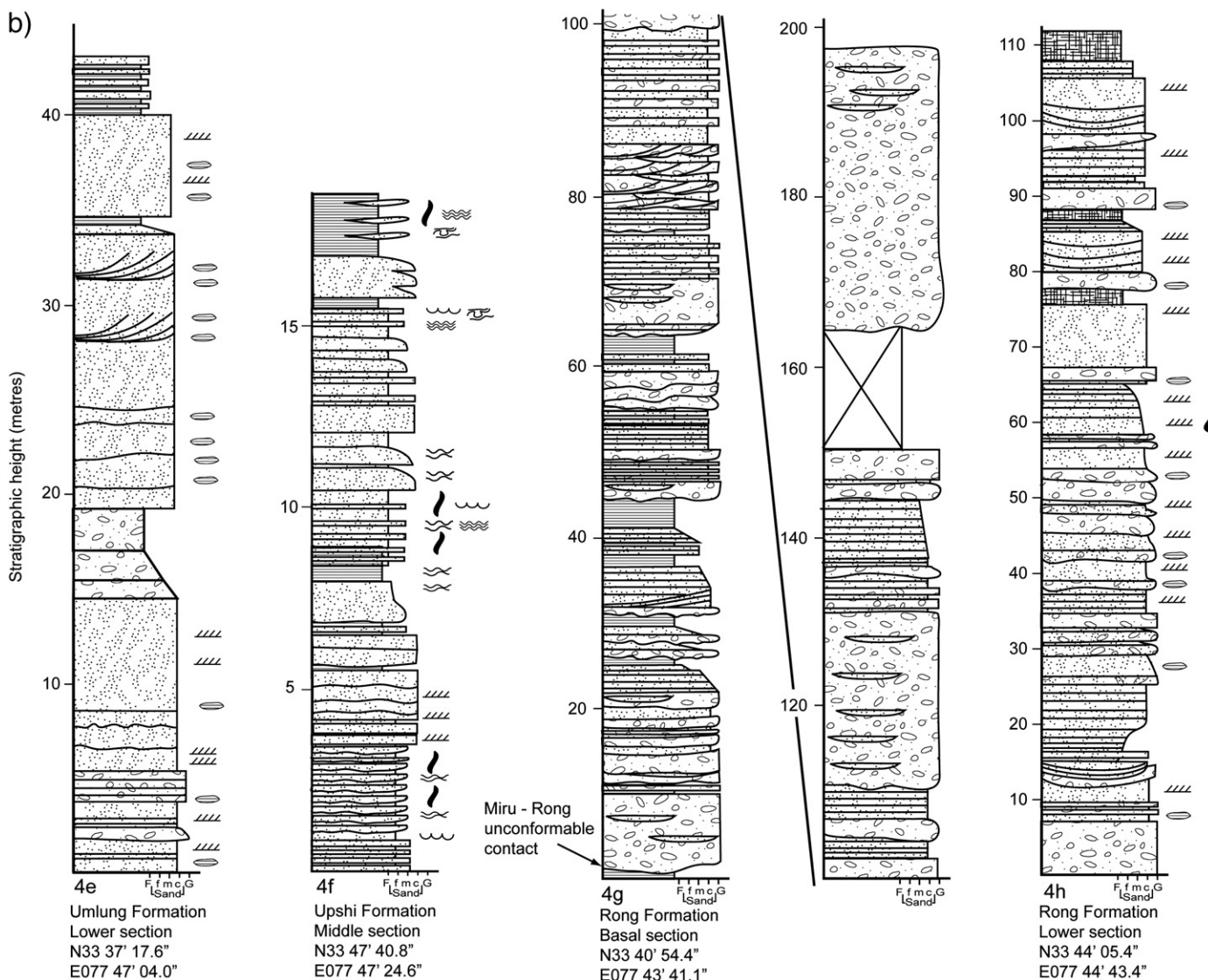


Fig. 4 (continued).

The upper section of the Upshi Formation (Table 1, Fig. 5h) is characterized by a decrease in overall grain size; fine grained red-brown sandstones and red mudstones dominate, with the rare occurrence of pebble conglomerates.

4.1.6. Rong Formation

Outcropping between the villages of Miru and Lato, observed at both Lato and Miru to sit unconformably above the Tar Group's Miru Formation (contacts described in Section 4.1.1), exists what we have termed the Rong Formation, which Clift et al. (2002) considered to be the Chogdo Formation. We provide the reasons for our alternative assignment in Section 4.5 and Table 2. The Rong Formation in the Upshi–Lato section is characterized by red–green sandstones, coarse, angular lithic arenites associated with conglomerates and red and blue shales, all of which are folded into a large NW–SE trending syncline between Miru and Lato (Figs. 3, 4g–h, and 5i). Detailed sedimentology including sedimentary structures is given in Table 1. Flute and gutter casts, which are the sedimentary structures most likely to be associated with major flow direction, show palaeoflow to the north-west (Fig. 6).

4.1.7. Lato Formation

Comprising a relatively small outcrop directly to the west of the village of Lato exists a sedimentary succession which we have termed the Lato Formation. The Lato Formation is tectonically bound to the north by the Miru Formation, and the south by the Lamayuru Formation. It is composed of breccias, conglomerates, immature sandstones, and well cleaved blue and red shales and mudstones (Fig. 4i). Sedimentary structures are detailed in Table 1. Flute and gutter casts (Fig. 5j) give a tectonically restored west-north-west palaeoflow direction (Fig. 6).

4.2. Geochemical characteristics of the Formations

4.2.1. Mudstone geochemistry

Henderson et al. (2010b) and Garzanti and van Haver (1988) explored trace element composition of IBSR mudstones as a method to determine the varying concentrations of trace element contribution from ultramafic/ophiolitic sources throughout the stratigraphy. The combination of these two studies showed that in the Zaskar Gorge type section only the younger IBSR formations of the Indus Group (e.g.

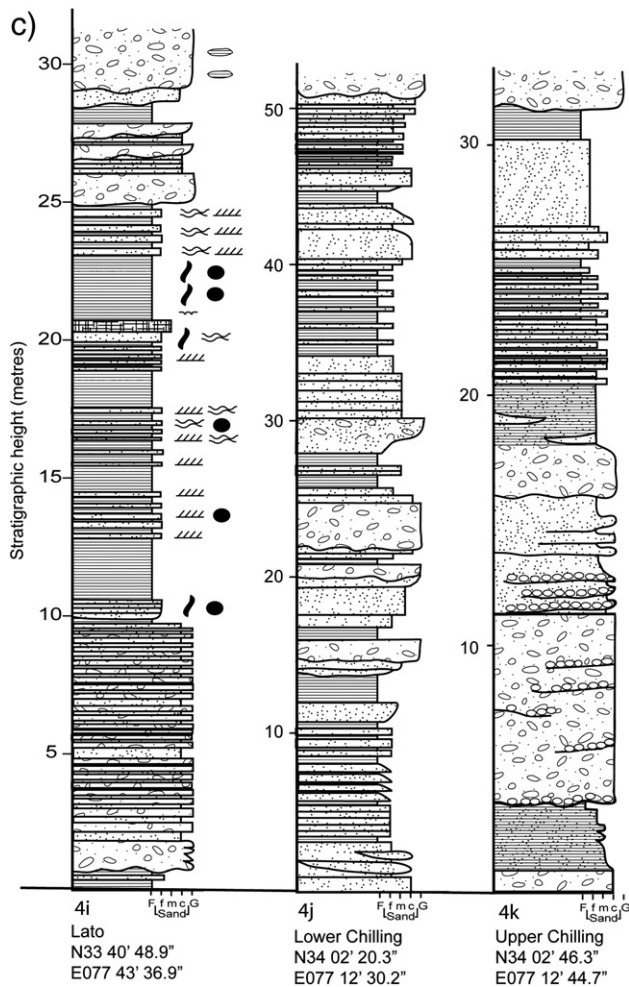


Fig. 4 (continued).

Choksti Formation) show enrichment in Cr and Ni relative to Post Archean Australian Shale (PAAS) values, whereas older IBSR rocks from the Tar Group and Lower Indus Group are not enriched relative to PAAS (Fig. 8). This creates a potential way of assigning an IBSR rock of unknown depositional age, with a corresponding relative stratigraphic height, although more analyses are necessary for robust interpretation.

X-ray fluorescence (XRF) analysis was conducted on six mudstone samples collected from various formations throughout the Lato–Upshi field area. In addition, three samples from the precollisional Indian passive margin Lamayuru Formation were analyzed. Sample preparation and XRF analytical procedures closely followed those outlined in Ramsey et al. (1995) and Watson (1996), and full XRF results are available in Section S1 of the Supplementary data. Gongmaru La, Rong and Miru Formations all display values comparable with both Indus Group and Indian Passive margin values. The Lato Formation has values higher than any IBSR or Lamayuru rocks.

4.2.2. Sandstone petrography

Sandstone petrographic studies conducted on samples from the IBSR along the Zaskar Gorge (Garzanti and van Haver, 1988; Henderson et al., 2010b) have provided a framework for characterizing IBSR formations, showing that there is a gradual evolution in petrography from undissected to dissected arc provenance through time. A total of 10 sandstone samples from our field areas were thin sectioned and analyzed by point-counting using the Gazzi–Dickinson method (Ingersoll et al., 1984; Dickinson, 1985). For each sample >100 orderly spaced points were counted and results are presented in

a provenance discrimination plot based on quartz, feldspar, and lithic proportional composition (Dickinson and Suczek, 1979; Fig. 9), with full results available in Section S2 of the Supplementary data.

The analyzed quartz, feldspar and lithic clast compositions of IBSR samples from the Upshi–Lato section imply that sediment was sourced from a progressively dissected arc, and petrographically resembles IBSR rocks along strike in the Zaskar Gorge (Fig. 9). The composition of the older, underlying Miru Formation plots in the Transitional Arc provenance field, similar to the Tar Group in the Zaskar Gorge. Younger Indus Group samples dominantly plot in the Dissected Arc provenance field, similar to the Indus Group formations in the Zaskar Gorge. For all IBSR samples in the Lato–Upshi section, lithic clasts are dominantly of volcanic origin, and detrital muscovite (see Section 4.2.5) is present in all formations except the Miru, Gonmaru La and Artsa formations.

The petrography of IBSR rocks compared to the Lato Formation is notably different. Sandstones from the Lato Formation plot within the Recycled Orogen field (Fig. 9). These samples contain an absence or very low abundance of feldspars, and lithic clasts are dominantly of sedimentary type. Chert and carbonate clasts occur in greater abundance than in the IBSR samples, and grains of serpentinite and peridotite are not apparent. Detrital white micas, metamorphic psammites, and rare volcanic lithic clasts are also present.

4.2.3. Conglomerate clast counts

A series of clast counts were conducted on conglomerates throughout the field area and results are presented in Fig. 10. Conglomerate clasts typical of IBSR formations (as identified in the type section of the Zaskar Gorge by Henderson et al., 2010b) are present in all of the Indus Group formations analyzed in the Lato–Upshi section. Granitoid clasts are abundant in all three Indus Group Formations, alongside the occurrence of ultramafic igneous, clastic sedimentary, and chert clasts. However, basalt, other volcanic, and quartzite clasts are absent in the Umlung Formation. Non-autogenic limestone clasts are only present in small abundances in the Rong Formation. Notably, we also observed clast composition to vary quite significantly on a local scale.

Breccias and conglomerates from the Lato Formation are dominant in sedimentary lithic, chert, and quartzose clasts. Also present are limestone and quartzite clasts. A very minor amount of granitoid and basalt clasts also occur.

4.2.4. $^{206}\text{Pb}/^{238}\text{U}$ dating of detrital zircons

U–Pb isotopic age dating of detrital zircons from four strategically selected samples from our field areas was conducted using Laser Ablation–MultiCollector–Inductively Coupled Plasma Mass Spectrometry (LA–MC–ICPMS) at the Natural Environment Research Council Isotope Geoscience Laboratories (NIGL), at the British Geological Survey. Full details of sample preparation and analytical procedure are given in Section S3a of the Supplementary data, alongside full sample and standard results available in S3b of the Supplementary data. Blank-corrected measured data were fed from the mass spectrometer into a NIGL developed Excel© sheet and Isoplot (Ludwig, 2003) was used for age calculation and data presentation. Histograms displaying the $^{206}\text{Pb}/^{238}\text{U}$ ages of the samples compared to a compilation of zircon ages from both Indian and Eurasian plate sources are displayed in Fig. 11.

Sample LT07060 from the Indus Group's Rong Formation is dominated by Cretaceous–Early Cenozoic aged detrital zircons, typical of IBSR rocks as characterized in the Zaskar Gorge (Fig. 11, Wu et al., 2007; Henderson et al., 2010b), with only two older grains of 210.8 (± 6.0) Ma & 528.1 (± 14.7) Ma. In addition to Cretaceous–Early Cenozoic grains, an abundance of Precambrian grains were analyzed from the lowermost Tar Group's Miru sample (LT07062), whereas the younger Miru sample (LT07005) contained only three Precambrian grains.

In contrast to IBSR samples, the Lato Formation sample is dominated by older Paleozoic and Precambrian aged assemblages, with only a rare, subordinate proportion of younger grains. Lato Formation sample LT07058 contained only two young ages of 51.1 (± 0.7) Ma and 76.7 (± 1.1) Ma.

4.2.5. $^{40}\text{Ar}/^{39}\text{Ar}$ dating of detrital white micas

Detrital white mica $^{40}\text{Ar}/^{39}\text{Ar}$ ages were obtained from grains from two medium grained sandstone samples from the Upshi Formation, one sample from the Lato Formation, and three modern river sands; one from a river catchment draining the Indian plate Tethyan and

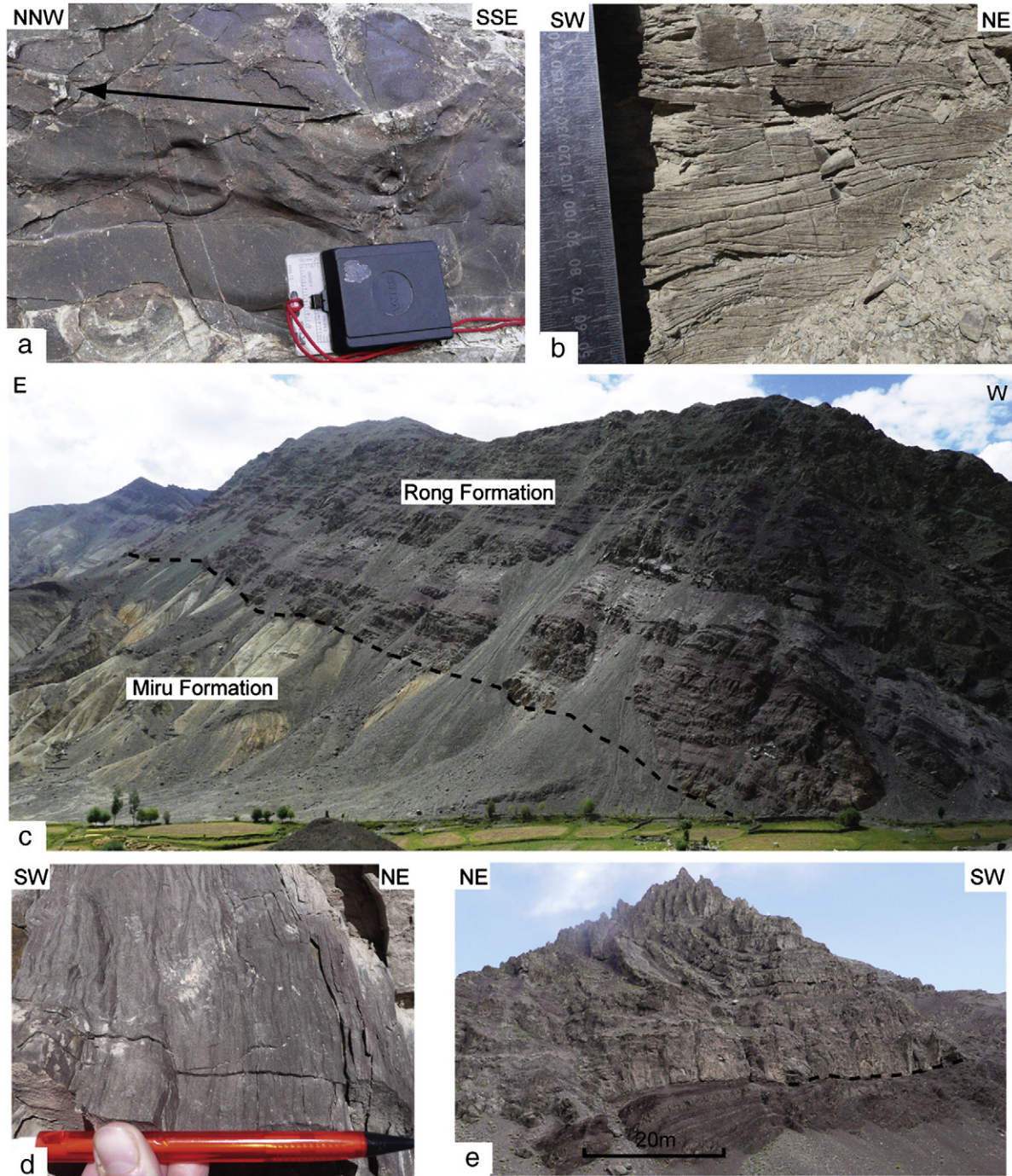


Fig. 5. Field photos (Lato-Upshi section, Field area 1). (a) Current crescent from the Miru Formation. Arrow indicates flow direction. Taken from N 33° 44' 44.1", E 077° 45' 18.8". (b) Hummocky cross lamination within the Miru Formation. Taken from N 33° 44' 02.6" E 077° 45' 20.3". (c) Unconformable contact between Miru Formation and overlying Rong Formation, south of Miru village. Black dashed line depicts part of the contact. Taken from N 33° 44' 17.1, E 077° 44' 43.0". (d) Ripple lamination in the Gonmaru La Formation. Taken from N 33° 44' 57.1" E 077° 45' 32.5". (e) Stratigraphic contact between the Gonmaru La Formation and the overlying Artsa Formation. Dashed line depicts part of the contact. Taken from N 33° 46' 03.4" E 077° 45' 50.7". (f) Faulted contact between the Umlung and the Upshi Formations represented by the black dashed line. Transition from Lower to Upper sections of the Upshi Formation is marked by the black-white dashed line and based on the absence of coarse conglomerates in the Upper Upshi. Upward-coarsening cycles are visible in the Upshi Formation. Arrows depict younging direction. Taken from N 33° 47' 29.9" E 077° 47' 28.7". (g) Lower Upshi Conglomerate (See Section 4.2.3). Gr = granitoid, Ep = epidote, Ch = chert, Om = ophiolitic mélangé, Bs = basalt, Lst = Limestone. Taken from N 33° 47' 56.0" E 077° 47' 36.3". (h) Sediment deformation in Upper Upshi sandstone bed. Taken from N33° 47' 29.9" E 077° 47' 28.7". (i) Channel shaped sand bodies within the Rong Formation. Beds young towards the NE. Taken from N 33° 41' 22.80" E 077° 44' 14.31". (j) Gutter casts within the Lato Formation. Taken from N 33° 40' 47.9" E 07° 43' 35.9".

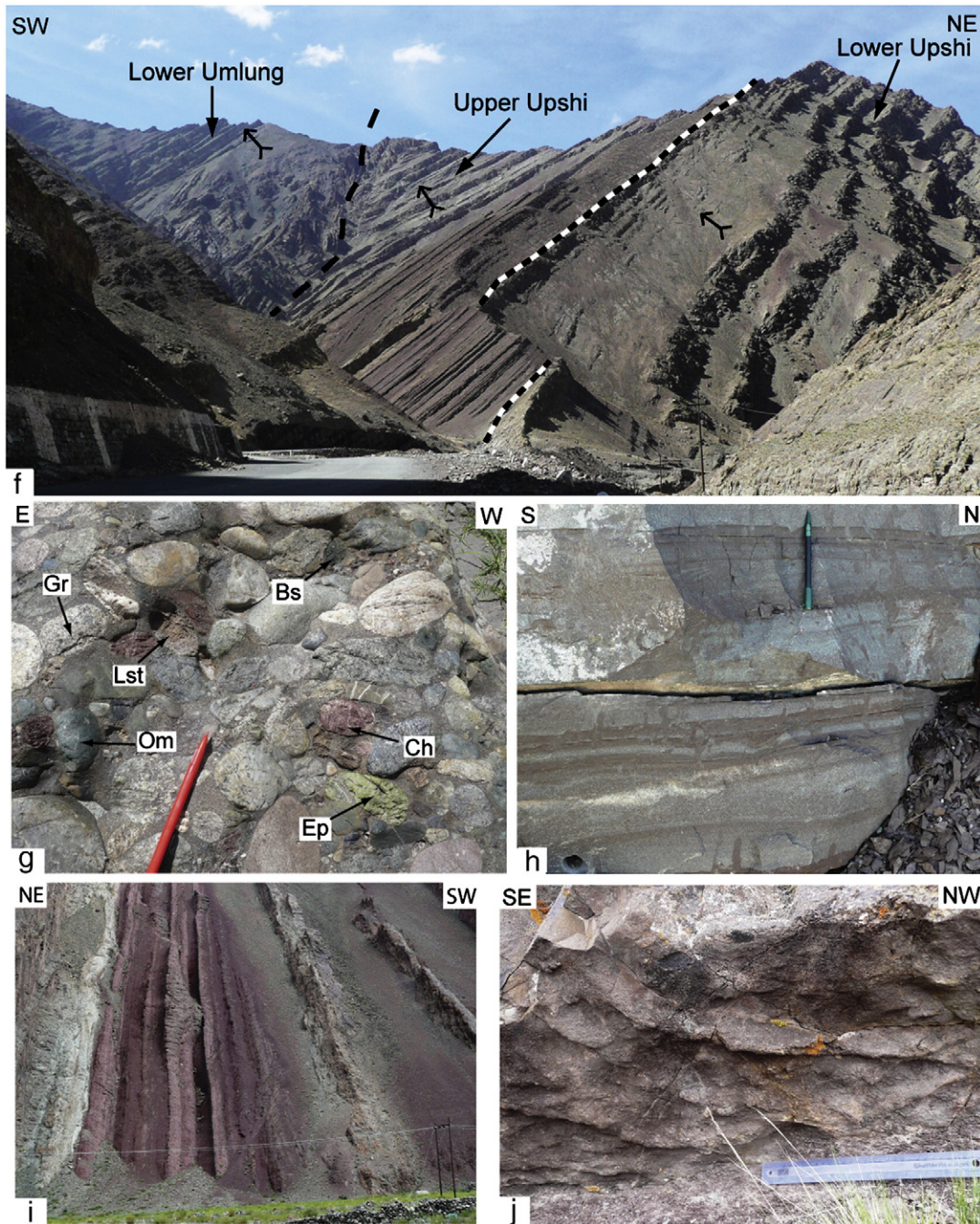


Fig. 5 (continued).

Higher Himalaya, and the other two draining the Lhasa Block and Trans-Himalaya of the Asian southern margin. Sandstone samples were crushed to gravel and sand sized grains using standard rock crushing techniques at both Lancaster University and SUERC. Each sample was then sieved into 250–500 μm aliquots from which the micas were picked and then cleaned during a series of deionized water and then 5% HNO_3 ultrasonic baths. Mica grain sizes ranged from 200 μm to 300 μm . For each sample, mica grains were packed in approximately 6 mm diameter Cu-foil packages, stacked and interspersed with packages containing a mineral standard within quartz tubes. Further sample preparation details and analytical methodologies are available in Section S4 of the Supplementary data. Isotope

measurements were obtained using an ARGUS multi-collector mass spectrometer at the NERC Argon Isotope Laboratory, which is housed by the Scottish Universities Environmental Research Centre, Scotland (Mark et al., 2009).

$^{40}\text{Ar}/^{39}\text{Ar}$ ages are presented as probability density plots in Fig. 12. Raw data are available in Section S4 of the Supplementary data. Two distinct age groups were obtained from the Lower Upshi sample (LT07025) comprising a 71.2 ± 0.7 to 78.4 ± 0.7 Ma population, and a younger 37.6 ± 0.4 to 45.9 ± 0.4 Ma population. The upper Upshi sample (LT07033), contains a single population of relatively young ages ranging from 24.4 ± 0.2 to 43.1 ± 0.4 Ma. These Eocene–Miocene ages are comparable to Cenozoic $^{40}\text{Ar}/^{39}\text{Ar}$ ages obtained from upper

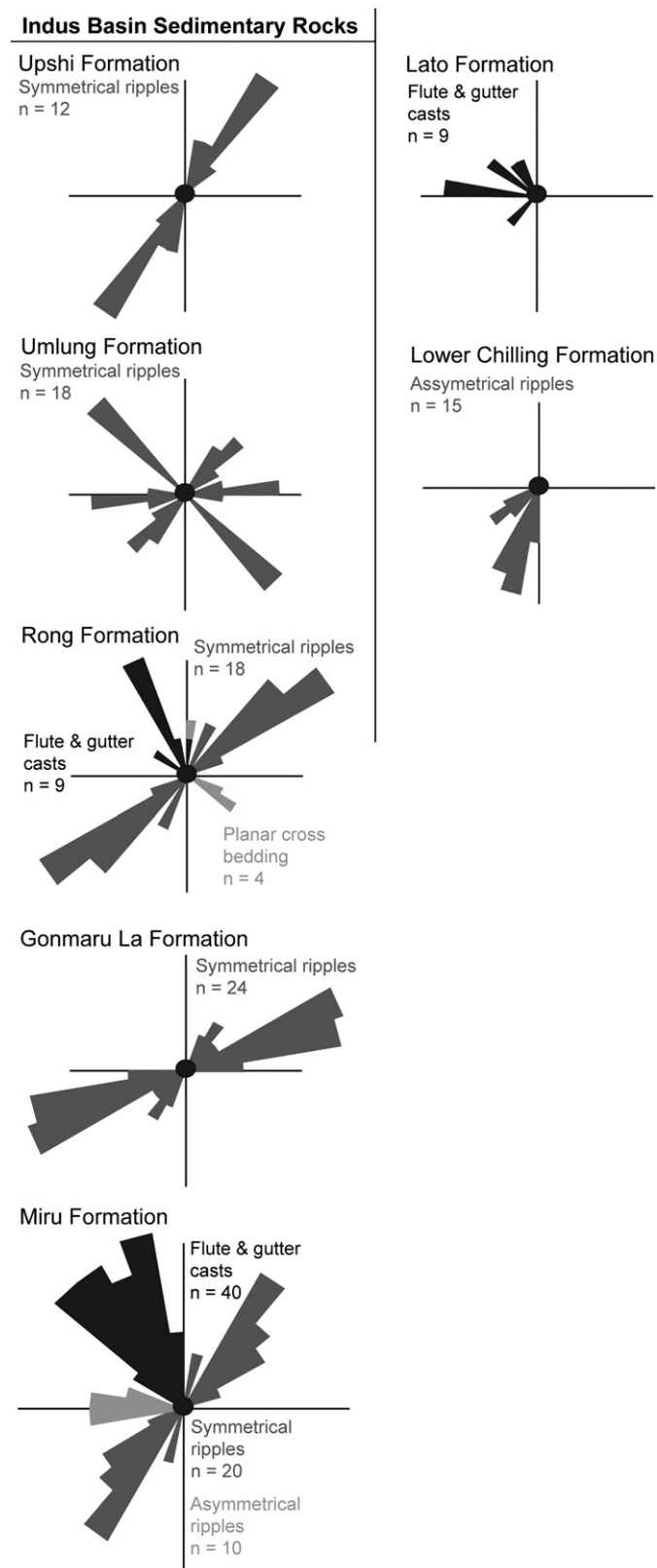


Fig. 6. Rose diagrams displaying tectonically restored measured paleocurrent indicators from the IBSR stratigraphy and Lato Formations (Field area 1: Lato–Upshi area, described in Section 4) and Chilling Formation (Field area 2, Chilling–Sumda area, described in Section 5), obtained from this study. Rose diagram section color shades correspond to the paleoflow feature written in matching color. Flute, gutter casts and cross-bedding most likely represent the direction of major channelled flow, asymmetrical ripples may represent deposition in an overbank environment, symmetrical ripples most likely represent wave movement in a marine or lacustrine shoreline environment.

Indus Group units of the in the Zaskar Gorge (Fig. 12, Henderson et al., 2010b).

Detrital white micas from the Lato Formation (LATO-09) reveal a much older age spectrum compared to the Indus Group samples with the dominance of grains yielding Mid Ordovician (468.8 ± 1.3 Ma) to Late Devonian ages (363.4 ± 1.3 Ma) (Fig. 12). Outlying from this dominant Paleozoic age population exists a single mica grain of Late Cretaceous age (67.2 ± 1.1 Ma); the youngest $^{40}\text{Ar}/^{39}\text{Ar}$ mica age identified in the Lato Formation.

4.2.6. Sm–Nd of detrital apatites

Studies using in-situ Sm–Nd isotopic analysis of detrital apatites have been demonstrated as a useful provenance discriminator tool, particularly for determining an Indian versus Eurasian plate provenance (Foster and Vance, 2006; Henderson et al., 2010a). We applied this method to analyze a medium grained sandstone from the Lato Formation (sample LT07058). Detrital apatites were obtained using standard crushing, grinding, and density separation techniques at the British Geological Survey. Apatites were mounted into epoxy resin mounts which were ground and polished, exposing fresh sections of the grains. Analysis by LA–MC–ICPMS was conducted at the University of Bristol, and followed the analytical procedures outlined in Foster and Carter (2007) and Foster and Vance (2006). A total of 20 apatites were analyzed and full sample and standard results are available in section S5 of the Supplementary data. Our results are displayed in Fig. 13 on a $^{147}\text{Sm}/^{144}\text{Nd}$ versus ϵ_{Nd} plot, where ϵ_{Nd} represents parts per ten thousand variation from CHUR of $^{143}\text{Nd}/^{144}\text{Nd} = 0.512638$ (Jacobsen and Wasserburg, 1980).

4.3. Detrital provenance

The stark contrast in both age and lithology between Indian and Eurasian plates (Section 2) allows for relatively straightforward provenance discrimination using the techniques described above. Whilst the Indian plate consists of Precambrian–Earliest Cenozoic sedimentary strata metamorphosed during the Cenozoic orogeny, the Eurasian plate consists of Jurassic–Cenozoic magmatic rocks intruded through Precambrian–Mesozoic strata (Yin and Harrison, 2000). Thus, whilst zircons from the Indian plate will be dominated by grains of Precambrian U–Pb age, Eurasian-derived grains will be dominantly, although not exclusively, of Mesozoic–Cenozoic age. White micas with Cenozoic Ar–Ar age are typically representative of the metamorphism associated with the Himalayan orogeny on the Indian plate; white mica is uncommon in the Trans-Himalaya but grains with Late Miocene–Pliocene ages are found in rivers draining the southern margin of the Asian plate (Fig. 12 bottom panel). Whilst the signature of ophiolitic input, expressed in petrography and mudstone geochemistry, may be the result of Eurasian (associated with the Dras arc complex) or Indian (Spongtag) derivation, magmatic Asian versus sedimentary/metamorphic Indian plate input can be clearly differentiated in conglomerate and sandstone petrography and the Sm–Nd composition of apatites (Fig. 13, left hand histogram and right hand scatter plot on which Indian and Asian fields are delineated).

4.3.1. Provenance of the Indus Basin sedimentary rock formations

The undissected to dissected arc sandstone petrographic signature (Fig. 9) and high proportion of granitoid conglomerate clasts (Fig. 10) throughout the stratigraphy, coupled with the abundance of Jurassic–Paleogene aged detrital zircons from both the Miru and Rong Formations (Fig. 11), suggests that sediment was largely sourced from the Trans-Himalayan arc on the Eurasian margin which was undergoing progressive dissection and uplift (Fig. 9) during Early–Mid Cenozoic times, as expressed by the petrographic trend from undissected to dissected arc. We note the lack of agreement with our limited palaeocurrent measurements of NW-directed nature (Fig. 6),

Table 2

A summary of geological observations from both Clift et al. (2001, 2002) and this study, focused on the critical contacts for constraining collision at A) Lato (Field Area 1, section 4) and B) Chilling (Field Area 2, section 5). Note that two contacts, in different locations, are described in the Chilling field area, denoted in this table as a and b.

A	Critical contact at Lato			
	Clift et al. (2001, 2002)		This paper	
			Interpretation	Reasoning
Fm. above contact	Eurasian-derived Chogdo Fm. of Tar Group (50.8–51 Ma)		Eurasian derived Rong Fm. of Indus Group (<48.4 Ma; probably ~Oligocene age)	
Contact	Unconformity		Tectonized unconformity	
Fm. below contact	Indian margin Lamayuru Fm.		Eurasian derived Miru Fm. of Tar Group	
Evidence for collision?	Eurasian detritus deposited on Indian plate by 51 Ma, constraining collision to have occurred by this time		No constraint to the timing of collision is possible at this location since the geology shows younger Indus Group unconformably overlying older Eurasian derived Tar Group	
B	Critical contact at Chilling			
	Clift et al. (2001, 2002)		This paper	
			Interpretation	Reasoning
Fm. above contact	Eurasian-derived Chogdo Fm. of Tar Group (50.8–51 Ma)		Indian-derived Upper Chilling Fm	
Contact	a/b. Unconformable		a. Conformable	b. Tectonized/obscured
Fm. below contact	a. Indian Margin Lamayuru Fm.	b. Ophiolitic mélange	a. Lower Chilling Fm.	b. Ophiolitic mélange
Evidence for collision	Eurasian detritus deposited on Indian Plate by 51 Ma, constraining collision to have occurred by this time.		Since the overlying formation consisting of Indian-derived material cannot be correlated with the Chogdo Formation, timing of collision cannot be constrained since 1) Eurasian detritus is not overlying Indian Plate material, and 2) no accurate age constraints currently exist for the deposition of the Upper Chilling Formation	

which we attribute either to the highly deformed nature of the rocks, which impedes accurate palaeocurrent reconstruction, or a palaeogeography as outlined in Section 4.6. A greater detrital contribution from ultramafic igneous sources (e.g. ophiolite) in upper IBSR stratigraphic levels, is suggested by the enriched Cr and Ni mudstone concentrations in the Rong and Gonmaru La Formations (Fig. 8).

The older detrital zircons from the Miru Formation may be derived from either an Indian Plate or Eurasian derived Lhasa Block provenance (Fig. 11). $^{40}\text{Ar}/^{39}\text{Ar}$ white mica ages obtained from the Upshi Formation show similar age affinities to those of Indian plate provenance (sample ZANSK-2; Fig. 12). The confinement of detrital white micas to upper IBSR levels (e.g. Rong Formation, Upshi Formation), coupled with conglomerate clast diversity in these formations showing the addition of non-autogenic limestones and quartzite clasts likely derived from the Indian passive margin (Fig. 10) is the first unequivocal evidence of Indian Plate derived input into the otherwise dominantly Eurasian derived IBSR.

4.3.2. Provenance of the Lato Formation

The results of our field and laboratory analysis have revealed that the Lato Formation is distinctly different from the IBSR of both the Lato–Upshi section and Zaskar Gorge. Sandstone petrography reveals that the Lato sandstones were derived from a Recycled Orogen provenance (Fig. 9; as defined by Dickinson and Suczek, 1979)

as opposed to a Transitional-Dissected Arc provenance for IBSR sandstones (Section 4.2.2). Cr and Ni concentrations for Lato Formation mudstones are significantly enriched compared to IBSR samples (Fig. 8, Section 4.2.1), and igneous clasts such as granitoid, volcanic, and ophiolitic clasts, occur in significant quantities in all IBSR formations (Fig. 10; Section 4.2.3), in contrast to the Lato Formation where clasts are dominantly of sedimentary origin. Isotopic analysis points towards an Indian Plate detrital provenance for the Lato Formation, with a dominance of Precambrian and Early Paleozoic U–Pb detrital zircon ages (Fig. 11, Section 4.2.4) combined with a dominant array of Mid Ordovician to Late Devonian detrital mica $^{40}\text{Ar}/^{39}\text{Ar}$ ages (Fig. 12, Section 4.2.5). These were likely derived from Indian Plate granitoid intrusions; e.g. the Upper Ordovician Nyimaling granite (Stutz and Thöni, 1987), presently exposed only 10 km from the Lato Formation (Fig. 1). Sm–Nd results of detrital apatites from the Lato Formation also suggest that sediment was dominantly sourced from an Indian Plate origin with reference to the provenance fields as defined in Henderson et al. (2010a) and from published bulk rock Sm–Nd data (Fig. 13; Section 4.2.6). These data contrast with those from the IBSR in which detrital zircon U–Pb ages are dominantly derived from the Trans-Himalaya (Fig. 11), detrital white mica ages are much younger of dominantly Cenozoic High Himalayan age (Fig. 12), and detrital apatites from the IBSR in the Zaskar Gorge are entirely Eurasian-derived (Henderson et al., 2010a).

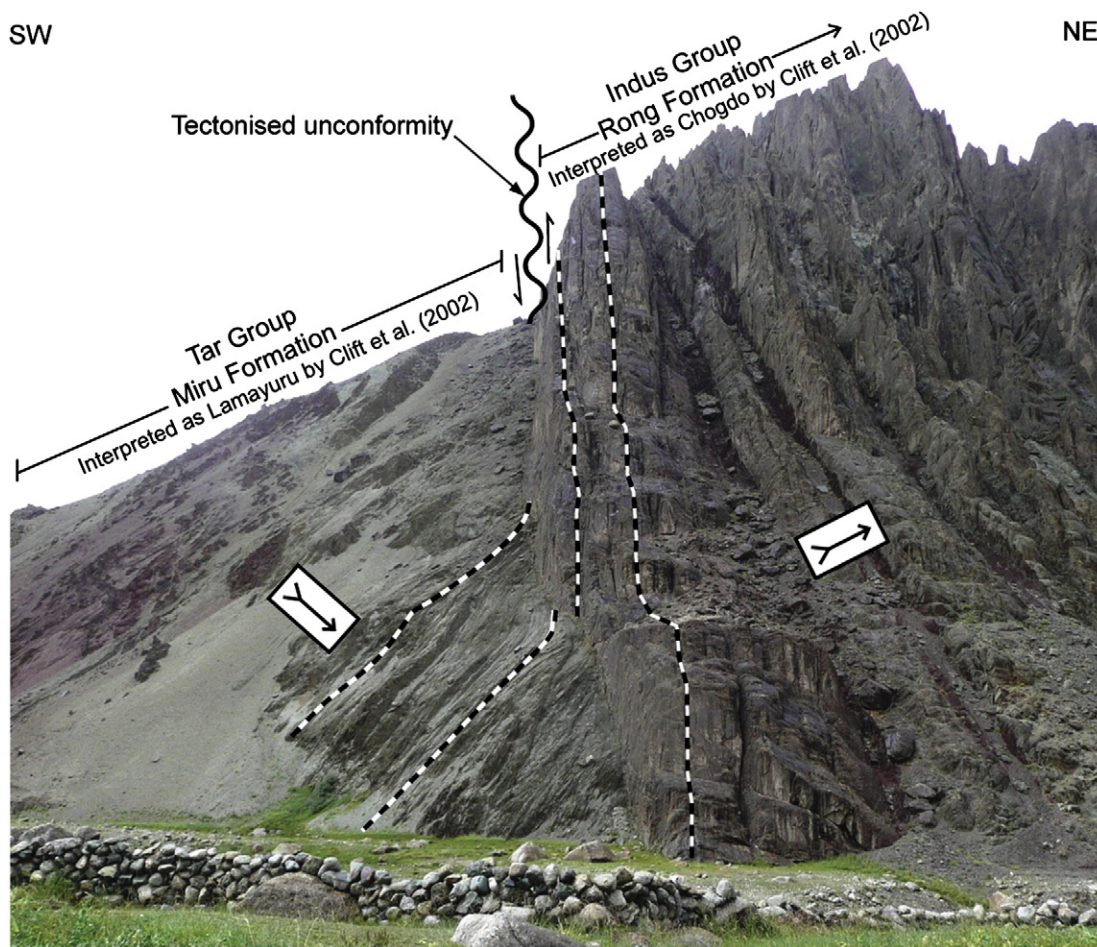


Fig. 7. Miru–Rong Formation contact taken from the village of Lato at N 33° 40' 54.4" E 077° 43' 41.1". Dashed black lines depict bedding planes. Arrows indicate younging direction. See text in Section 4.1.1 for description and Section 4.5 and Table 2 for explanation.

Although the absence of Cenozoic mica grains might suggest a pre-collisional India provenance for the Lato Formation, a 51.1 (± 0.7) Ma zircon grain constrains the depositional age at younger than this time. Post-collisional deposition is also supported by the input of two apatite grains with Eurasian affinity (Fig. 13). However, we recognize that the number of grains used to support this conclusion is small. Thus we consider the deposition of the Lato Formation may post-date India–Eurasia collision, but more analyses are required to verify this. We conclude that Indian plate sediments, some locally derived, were transported in a WNW direction (Fig. 6) during (at least) the incipient phases of India–Eurasia collision, possibly incorporating a minor amount of Eurasian plate material into the detritus. Thus, the nature of the Lato Formation is clearly diversely different to the IBSR stratigraphy which is dominated by detritus of Eurasian affinity.

4.4. IBSR stratigraphic correlation

Based on the facies and geochemical characteristics presented above, we suggest possible correlations between the stratigraphy exposed along the Upshi–Lato transect to that of the IBSR “type-section” exposed in the Zaskar Gorge further west (Fig. 2).

4.4.1. Correlation of the Miru Formation with the Tar Group in the Zaskar Gorge

The suggested prograding deltaic deposits of the Miru Formation (Table 1) may represent the eastern equivalent of marginal marine

deposition of the Upper Tar Group in the Zaskar Gorge, deposited during the demise of the Neo-Tethys. The youngest U–Pb detrital zircon age of 54.3 (± 8.0) Ma obtained from Miru Formation sample LT07062 (Fig. 11) is consistent with the widely considered Early Eocene depositional age for the upper Tar Group (Green et al., 2008; Henderson et al., 2010b). Furthermore, sandstone petrographic analysis of the Miru Formation is similar in composition to Tar Group samples, plotting in the lower Transitional Arc field (Fig. 9; Garzanti and van Haver, 1988; Henderson et al., 2010b). We acknowledge however, that the mudstone trace element concentrations of Cr and Ni (Fig. 8) in the Miru Formation have higher values than Tar Group samples from the Zaskar Gorge (Henderson et al., 2010b) resembling more the values of Indus Group and Indian plate Lamayuru formations. The absence of preserved conformable stratigraphy above the Miru Formation and presence of an unconformable contact with the overlying Rong Formation in the central and southern areas of the Upshi–Lato section suggest that a significant part of the IBSR record could be missing from this section (Fig. 2).

4.4.2. Correlation of the Gonmaru La, Artsa, Umlung, Upshi and Rong Formations with Indus Group rocks of the Zaskar Gorge

We suggest these units may equate with the Zaskar Gorge <49.4 Ma Indus Group (Fig. 2), rather than the Tar Group, with which they show dissimilarity in terms of their quartzo-feldspathic rich nature of sandstones, enriched Ni and Cr concentrations and, for the upper units, micaceous content.

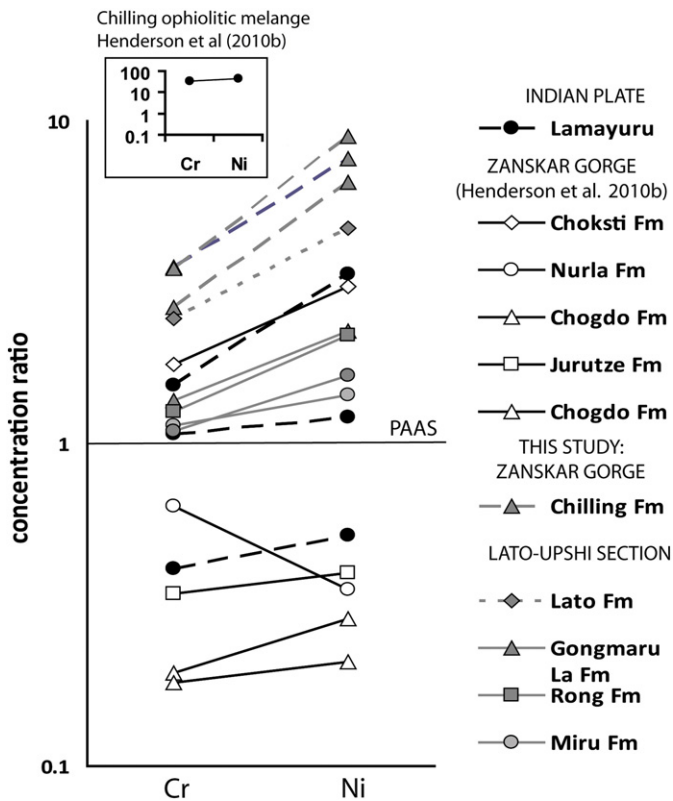


Fig. 8. XRF results showing selected trace element concentrations from five IBSR shale samples and one Lato Formation shale sample from Field Area 1: Lato–Upshi area, described in Section 4 (see Section 4.2.1), three Chilling Formation shale samples from Field Area 2: Chilling–Sumda area, described in Section 5 (see Section 5.2.1) and Lamayuru Formation data. Concentrations are normalized to trace element concentrations of Post Archean Australian Shale (PAAS) compiled by Taylor and McLennan (1985); where (in ppm) Cr = 110, Ni = 55. Data from the Chilling ophiolitic Melange (Section 5.1.4), and Indus Group samples collected along the “type section” in the Zanskar Gorge from Henderson et al. (2010b) are also plotted.

We propose that the Gonmaru La Formation may be a lateral equivalent to the Indus Group’s Choksti Formation’s Red Shale Member in the Zanskar Gorge, based on very similar fine facies composed of distinctive red shales and subordinate red sandstones. Further to this, the overlying non-micaceous Artsa Formation consisting of upward-fining sedimentary cycles displays very similar facies characteristics to the Choksti Formation’s Middle Sandstone unit in the Zanskar Gorge.

The presence of detrital white micas and non-autogenic limestone clasts in the Umlung, Upshi, and Rong Formations suggests correlation of these units to the Choksti Formation’s Upper Sandstone Member and the Nimu Formation in the Zanskar Gorge, interpreted as axial river deposits of the palaeo-Indus (Henderson et al., 2010b). However, the fluvial facies observed in the upper stratigraphic units of the Indus Group in the Zanskar Gorge are likely representative of a more downstream-evolved axial river system compared to what is recorded further east in the proposed alluvial facies of the Upshi–Lato section (Fig. 2, Table 1).

Within the Upshi–Lato section, based on similar facies and micaceous composition with a transitional arc provenance, we equate the southern outcropping Rong Formation to represent a similar stratigraphic level to the northerly located Upshi and Umlung Formations. Our decision to differentiate between a northern and a southern stratigraphy for the upper Indus Group is based on the lack of direct correlation available between the Upshi/Umlung Formation and the Rong Formation.

Unlike the Chogdo Formation exposed in the Zanskar Gorge, with which the Rong Formation has previously been correlated (Clift et al.,

2002), the Rong Formation is not observed to be related above or below to fossiliferous limestone units (of the Sumda and Nummulitic Limestone Formations). Clift et al. (2001, 2002) describe the Chogdo Formation as consisting of “dark, red-purple weathering series of interbedded sandstones, siltstones and mudstones, as well as minor conglomerates”. We consider this description to also be applicable to other IBSR of higher stratigraphic levels and correlate the Rong Formation to higher stratigraphic levels of the IBSR, as argued above and further in Section 4.5.

4.5. Examining evidence for India–Eurasia collision from the Upshi–Lato section (Table 2)

Using the data presented above, we assess the validity of the stratigraphic contact used by Clift et al. (2002) to constrain the time of India–Eurasia collision. It is at the village of Lato where Clift et al. (2002) considers Eurasian derived Chogdo Formation (dated at 50.8–51 Ma in the Zanskar Gorge) to unconformably overlie Indian passive margin sediments of the Lamayuru Formation, thus defining a minimum age of collision (Table 2). Here we discuss (1) the nature of the contact, (2) whether the red beds above the contact belong to the Chogdo Formation and (3) whether the rocks below the contact are of Indian Plate origin.

Presented in Fig. 7 is a field photo taken from the village of Lato, interpreted by Clift et al. (2002) as representing the Tar Group’s Chogdo Formation unconformably overlying older, more deformed Indian Passive margin sediments of the Lamayuru Formation. In contrast to this, we interpret this contact as representing IBSR Indus Group sediments overlying IBSR Miru Formation (most probably correlated with the Tar Group – see Section 4.1.5) in what we have interpreted as a steeply-dipping tectonized angular unconformity. Our evidence for this interpretation is as follows:

In the underlying rocks SW of the contact (our IBSR Miru Formation, Clift’s “Lamayuru Formation” of the Indian plate), there is a dominance of young Eurasian derived U–Pb zircon ages (as young as 54.3 (±0.8) Ma from sample LT07062; see Fig. 11), a volcanic detritus enriched sandstone composition plotting in the Transitional arc provenance field (Fig. 9) and mudstone and sandstone facies showing a wealth of sedimentary structures (Section 4.1.1). These characteristics are typical of IBSR Formations (Section 4.3.1), and atypical of the Indian Plate Late Permian–Upper Cretaceous Lamayuru Formation as suggested by Clift et al. (2002), where one would expect a paucity of igneous detritus, abundance of sedimentary detritus, typical marine shale and limestone lithologies, (Robertson and Degnan, 1993) and Early Paleozoic–Precambrian detrital U–Pb zircon ages. Little description is provided by Clift et al. (2001, 2002) as to why these authors choose to assign this unit to the Lamayuru Formation. We suggest that their decision was made largely on the overall highly deformed fine grained nature of the rocks, and lack of apparent similar facies observed in any of the IBSR along the Zanskar Gorge. We however propose that this latter observation may be a result of lateral facies change.

Above the unconformity (to the NE) is a clastic sequence belonging to what we have termed the Rong Formation. In agreement with Clift et al. (2002) we assign this unit to part of the IBSR stratigraphy due to its Eurasian-derived signature (see Section 4.3.1). However, the presence of mudstones enriched in Cr and Ni concentrations (Fig. 8), limestone conglomerate clasts (Fig. 10), detrital white micas (Section 4.2.5), petrography with characteristics of a dissected arc provenance (Fig. 9), absence of interbedded limestones and the presence of a 48.4 (±1.4) Ma detrital zircon (Section 4.2.4; Supplementary Information S3b), makes the suggested correlation of this unit to the >50.8 Ma unmicaceous Chogdo Formation Tar Group (Clift et al., 2002), with its undissected arc petrography, unenriched Cr and Ni concentrations, and interbedded limestone beds, unlikely. Rather, as discussed in Section 4.4.2, we choose to correlate the Rong Formation

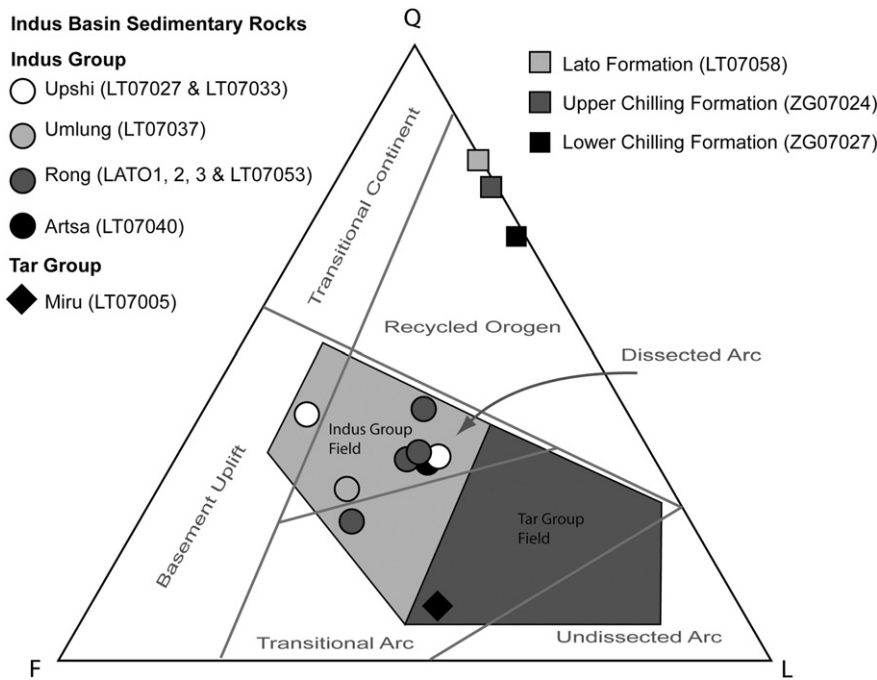


Fig. 9. Ternary diagram showing the varying proportions of quartz (Q), feldspars (F), and lithics (L) in Indus Basin and Lato Formation sandstones from Field area 1: Lato–Upshi area, described in Section 4 (see Section 4.2.2) and Chilling Formation sandstones from Field area 2: Chilling–Sumda area, described in Section 5 (see Section 5.2.2), based on point counting results. Provenance fields are determined from Dickinson and Suczek (1979) and Garzanti and Van Haver (1988). Each point represents one sample. Typical Indus and Tar Group QFL proportions from the “type section” of the Zaskar Gorge, (Henderson et al., 2010b) are indicated.

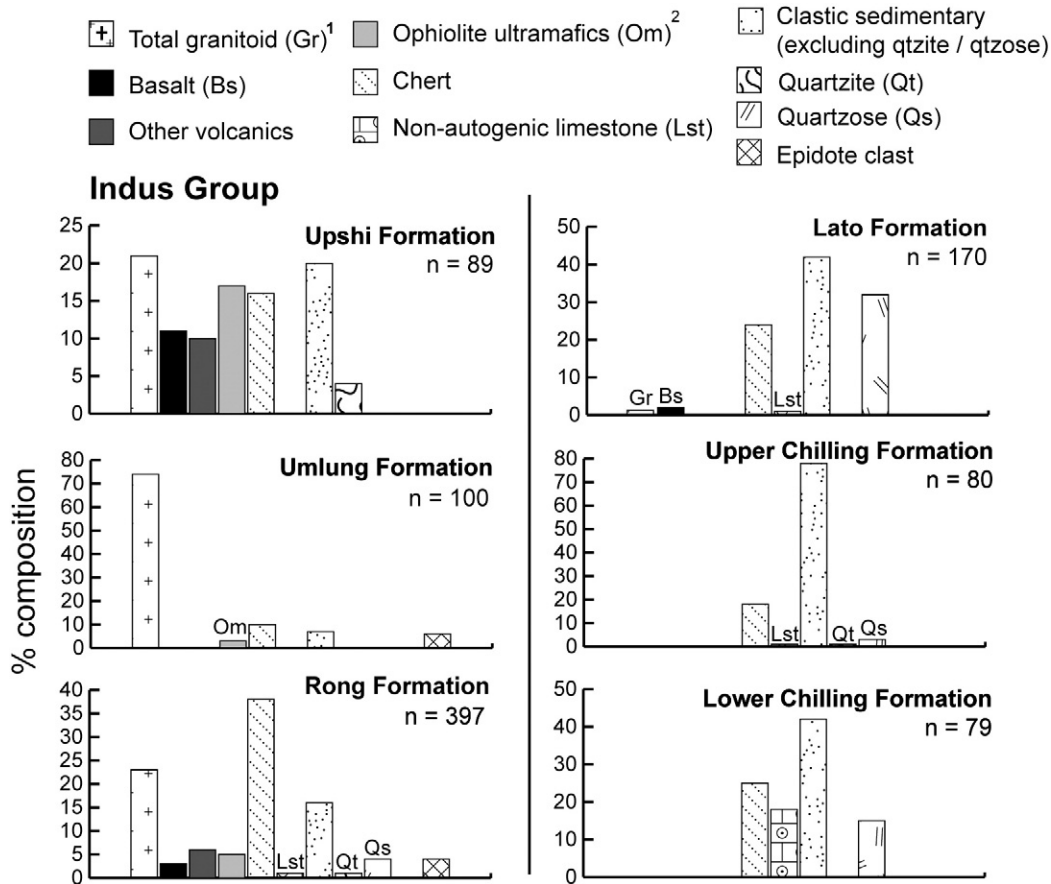
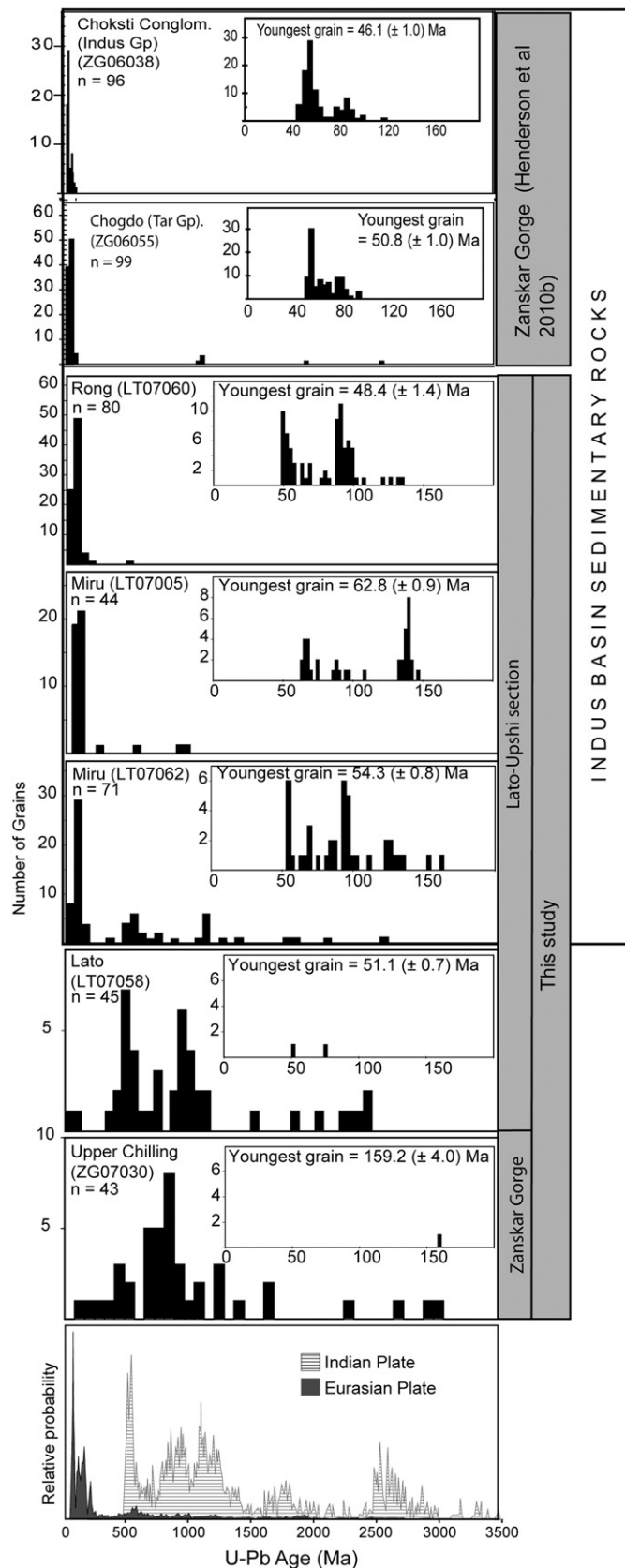


Fig. 10. Histograms displaying the changing proportions of conglomerate clast compositions as observed throughout the IBSR and Lato Formations in Field Area 1: Lato–Upshi area, described in Section 4 (see Section 4.2.3) and Chilling formation of Field Area 2: Chilling–Sumda area, described in Section 5 (see Section 5.2.3). ¹Includes all forms of granite. ²Peridotites, serpentinite, mafic–ultramafic plutonic rocks, and gabbro.

to a much younger Indus Group member; perhaps equivalent to the Upper Sandstone Member of the Choksti Formation or Nimu formations (as defined in Henderson et al., 2010b) on account of its similar petrography, white mica content, and mudstone geochemistry.



In summary (Table 2), we agree that this stratigraphic contact is indeed unconformable (and tectonized), however, rather than representing Eurasian derived Chogdo Formation overlying Indian Plate Lamayuru Formation, it more likely represents a break in deposition between the Lower and Upper levels of Eurasian derived IBSR sedimentation (Fig. 7). Furthermore, reassignment of the rocks north of the contact at this location from the older Tar Group (Chogdo Formation) to the younger IBSR Formations precludes this relationship from providing a tight constraint to the timing of India–Eurasia collision, regardless of the underlying substrate.

4.6. Suggested paleodepositional environment reconstruction for the IBSR

In order to accurately construct a palaeodepositional model with confidence, encompassing both the previously studied Zanskar Gorge location (Henderson et al., 2010b) and the Lato–Upshi section described in Section 4 above, ideally, high precision dating of the formations is required. In these rocks, accurate correlation between areas and detailed facies interpretations are precluded by a lack of high resolution dating, high levels of structural deformation in both field areas, and presumed rapid lateral facies variation. Our suggested reconstruction should be viewed in the light of these limitations.

In the Lato–Upshi section, the final transition from a marine to terrestrial environment of deposition is recorded in the suggested deltaic facies of the Miru Formation (dated at younger than 54.3 Ma ± 0.8 Ma from the youngest zircon grain; Section 4.2.4, Supplementary data S3b). Paleoflow indicators (Fig. 6) infer that delta progradation occurred in a west-north-westerly direction. With this proposed direction of delta progradation, marine depositional environments may have been more prolonged in more westerly areas, represented by sedimentation of the dominantly marine Tar Group further west (Fig. 2). The discontinuity of the Dras Arc towards the east (Fig. 1) suggests a likely transition from arc-bound deposition in western Ladakh (constrained by the Kohistan–Ladakh Island arc to the north and the Dras arc to the south; Henderson et al., 2010b) to evolving fore-arc to deltaic deposition of the Miru Formation in more eastern areas during the demise of the Neo-Tethys ocean. U–Pb ages of detrital zircons (Fig. 11) imply that sediment was dominantly derived from the Kohistan–Ladakh Island Arc to the north, however, a considerable number of Paleozoic and Precambrian aged zircons does not rule out a possible additional Indian Plate contribution (Fig. 14a).

The Middle-Eocene to ~Early Oligocene sedimentary depositional record is missing along the Upshi–Lato transect. We have correlated the alluvial deposits of the ~Mid Eocene–Miocene aged Gonmaru La, Artsa, Umlung, Upshi and Rong Formations, with the Choksti and Nimu Formations of the Zanskar Gorge, interpreted as axial-river deposits of the palaeo-Indus (Henderson et al., 2010b). This correlation, plus the likely presence of mixed Indian and Eurasian

Fig. 11. Histograms showing detrital zircon $^{206}\text{Pb}/^{238}\text{U}$ ages from three Indus Basin sedimentary rock samples, and one Lato Formation sample (Field Area 1: Lato–Upshi area, Manali–Leh Highway described in Section 4, see Section 4.2.4), and one Chilling Formation sample (Field Area 2: Chilling–Sumda area, Zanskar Gorge, described in Section 5, see Section 5.2.4). Two IBSR samples from the Chogdo and Choksti formations from the Zanskar Gorge stratigraphy (from Henderson et al. (2010b)) are also presented for comparison. “n” refers to the number of individual zircons analyzed per sample. Insets show detailed spread of Cenozoic to Jurassic ages. The bottom chart shows density plots of zircon $^{206}\text{Pb}/^{238}\text{U}$ ages characteristic of grains from the Indian Plate Tibetan Sedimentary Series and the Eurasian Plate. Indian Plate Tibetan Sedimentary Series data are from Gehrels et al. (2003), where n = 948. Eurasian plate data are compiled from Schärer et al. (1984), Xu et al. (1985), Murphy et al. (1997), Harrison et al. (2000), Miller et al. (2000), Chu et al. (2006), Leier et al. (2007), Wen et al. (2008), and Henderson et al. (2010b) where total n = 1323. Errors on all data are given at 2 σ (excluding the Indian Plate Tibetan Sedimentary Series from Gehrels et al. (2003) which is at 1 σ).

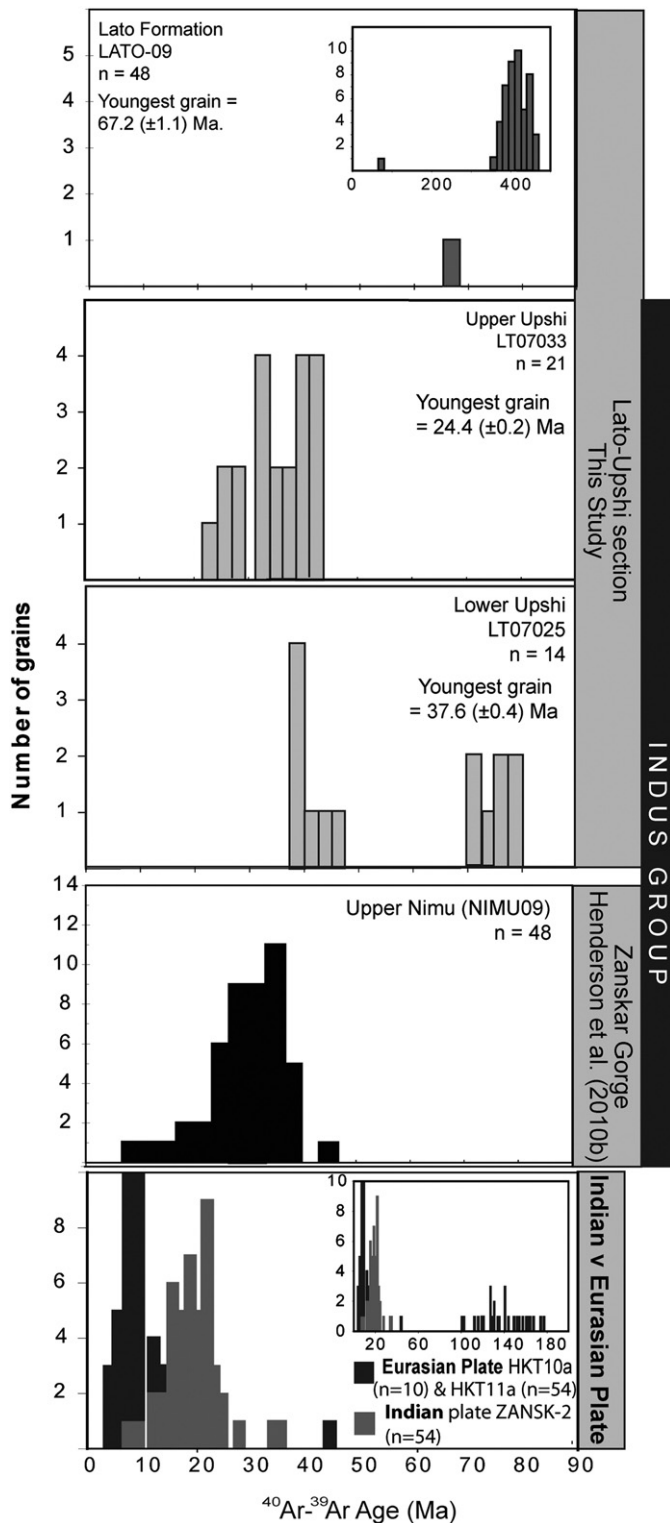


Fig. 12. Histograms displaying $^{40}\text{Ar}/^{39}\text{Ar}$ ages of detrital white micas from two Indus Group (Upshi Formation) samples and one Lato Formation sample. “n” refers to the number of mica grains analyzed per sample. A representative sample from the Indus Group (Nimu Formation) of the Zanskar Gorge, analyzed in Henderson et al. (2010b) is also shown for comparison. Youngest grain from each analysis is indicated. The bottom chart shows histograms of white mica $^{40}\text{Ar}/^{39}\text{Ar}$ ages characteristic of modern river sands draining the Indian Plate’s Tethyan and High Himalaya (ZANSK-2; Zanskar River) and the Eurasian Plate’s Lhasa Block and Trans-Himalaya (HKT10a and HKT 11a; Lhasa River and tributary thereof).

detritus in the Upshi and Rong Formations (Section 4.3.1), and evidence of NW-directed flow in the Rong Formation (Fig. 6), suggests that these upper stratigraphic levels of the IBSR of the Lato–Upshi section may represent an upstream equivalent to more evolved fluvial deposition of the axial paleo-Indus River which occurred at similar times further downstream as recorded in the Nimu Formations in the Zanskar Gorge (Fig. 14b).

The presence of a 24.2 ± 0.2 Ma detrital mica obtained from the Upshi Formation (Fig. 11) implies that Indus Group deposition occurred until at least the Late Oligocene times, in agreement with Sinclair and Jaffey (2001), Schlup et al. (2003) and Henderson et al. (Henderson et al., 2010b).

5. Field area 2: The Chilling–Sumda section, Zanskar Gorge

In the area surrounding the village of Chilling, Clift et al. (2001, 2002) identified Eurasian-derived IBSR Chogdo Formation, dated at 50–51 Ma, to unconformably overlie both Lamayuru Formation and also ophiolitic mélangé, both considered to be of Indian Plate affinity, thus constraining the timing of India–Eurasia collision at prior to 50 Ma. Using the same approach taken for the Lato–Upshi study described above, we used mapping, facies analysis, and geochemical characterization of units to determine the nature of the contacts and the assignment of formations above and below these contacts.

5.1. Stratigraphy and structure

As an extension to the geological mapping conducted by Henderson et al. (2010b) between the villages of Nimu and Sumda in the northern Zanskar Gorge, we present the results of our fieldwork between the villages of Sumda and Chilling (Fig. 15) which is the critical region to test the hypothesis of Clift et al. (2001, 2002).

5.1.1. Jurutze Formation

Outcropping along the road section for 4 km, ~1 km north of Chilling, the Jurutze Formation consists of black shales, siltstones, and gray phyllites with fine grained dark colored sandstones and carbonates present in the upper stratigraphic levels near to Sumda village (Table 3). The southern limit of the Jurutze Formation is fault bound just north of the village of Chilling against a red clastic sedimentary unit which we have termed the Upper Chilling Formation (see Section 5.1.3).

The Jurutze Formation is regarded as representing marine deposition in an outer-ramp to slope basinal environmental setting (van Haver, 1984; Garzanti and van Haver, 1988; Clift et al., 2002), probably within a basin bound by the Kohistan–Ladakh Island Arc to the north and the Dras Arc to the south, prior to Indian–Eurasia collision (Henderson et al., 2010b). Clift et al. (2001, 2002) considered the more southerly exposure of our identified Jurutze Formation to correlate with the Dras/Nindam Arc units. However, based on conformable relationships and similar facies, and in agreement with Searle et al. (1990), we believe that these rocks actually represent a southern continuation of the gray shales and phyllites of the Jurutze Formation.

5.1.2. Lower Chilling Formation

The lowermost stratigraphic levels of the Lower Chilling Formation crop out along the Zanskar–Markha River confluence, ~3 km south of the map in Fig. 15a, preserving a facies of dominant black–gray slaty shales, blue phyllites, and black crystalline carbonate limestones. The mid-upper stratigraphic levels are much coarser on average, consisting of mudstones, shales, fine to coarse sandstones, and breccias and conglomerates (Fig. 4j and 16a, Table 3). Limestone clasts are present in breccias and conglomerates (see Section 5.2.3) however, no visible fossils could be detected. Fuchs (1986) did however identify

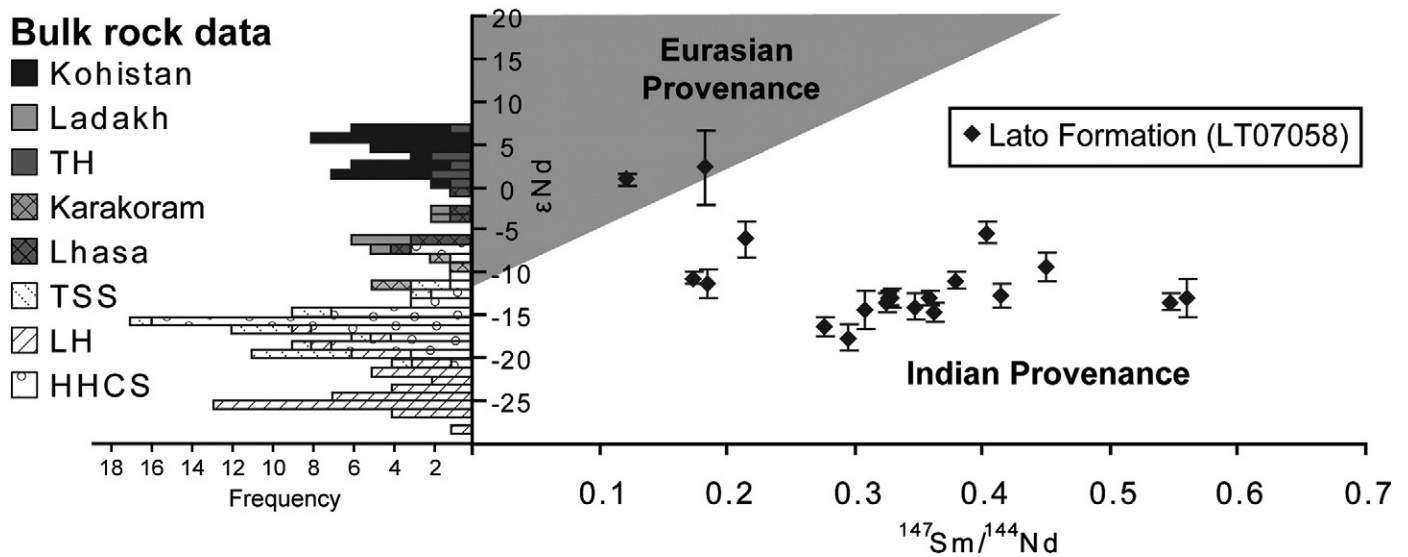


Fig. 13. Detrital apatite Sm–Nd isotopic results from a Lato Formation sand sample. Nd data is displayed in the form of ϵ_{Nd} ; $^{143}Nd/^{144}Nd$ variation from Bulk Earth (CHUR) in parts per 10,000. Where CHUR $^{143}Nd/^{144}Nd = 0.512638$ (Jacobsen and Wasserburg, 1980). ϵ_{Nd} error bars relate to 2 SE internal uncertainties, whereas the $^{147}Sm/^{144}Nd$ errors (2 SD) are not displayed on the plot but are always less than 0.002. Indian versus Eurasian provenance fields are displayed and based on the study of analyzing detrital apatites from both Indian and Eurasian modern river sediments by Henderson et al. (2010a). ϵ_{Nd} values from published bulk rock data are presented as a bar chart on the y-axis, with corresponding frequencies displayed on a separate x axis. Data sources for bulk rock data are as follows: Eurasian plate: TH (Trans-Himalaya) – Allegre and Othman (1980); Kohistan – Jagoutz et al. (2006), Khan et al. (1997), Petterson et al. (1993); Karakoram – Schärer et al. (1990); Lhasa Block – Debon et al. (1986); and Indian plate: TSS (Tibetan Sedimentary Series), HHCS (Higher Himalayan Crystalline Series), and LH (Lesser Himalaya) – Deniel et al. (1987), France-Lanord et al. (1993), Inger and Harris (1993), Parrish and Hodges (1996), Ayres (1997), Prince (1999), Whittington et al. (1999), Ahmad et al. (2000), and Miller et al. (2001).

limestone clasts containing *Nummulites* Sp., *Rotalia* Sp., and *Alveolinas* ex gr. determining the deposition of this formation to have been post middle Eocene. To the south, the Lower Chilling Formation is structurally juxtaposed against the Zanskar Supergroup; representing deposition on the northern continental margin of the Indian Plate (as described in McElroy et al., 1990).

5.1.3. Upper Chilling Formation

Sitting conformably above the Lower Chilling Formation, the base of the Upper Chilling is defined by a dominance of red lithologies, characterized by dark purple shales, fine-to-coarse red-purple silty-lithic arenites, and breccias and pebble conglomerates (Figs. 4k and 16b; Table 3). The northern extent of the Upper Chilling Formation is structurally bound against the Jurutze Formation. It is also internally faulted and associated with tectonic slices of the Chilling ophiolitic mélange (see Section 5.1.4). Its contact with the ophiolitic mélange on the hillside 2–3 km to the NW of Chilling is described in Section 5.1.4. It is this unit that Clift et al. (2002) considered to be Chogdo Formation; the reasoning why we disagree with this correlation, and do not correlate this unit with the Chogdo Formation is given in Section 5.4.

5.1.4. Chilling ophiolitic mélange

As recognized by several authors (Brookfield and Andrews-Speed, 1984; Fuchs, 1986; Searle et al., 1990; Fuchs and Linner, 1996; Clift et al., 2001, 2002) slices of tectonically emplaced sedimentary ophiolitic mélange outcrop around Chilling, consisting of dark green-black colored breccias (Fig. 16c), conglomerates, and sandstones (see Table 3 for a more detailed description of sedimentology). Fuchs and Linner (1996) also describe ophiolitic mélange of similar type outcropping around the village of Lato in the field area we describe in Section 4.1.7. A <3 m zone of deformation exists within the mélange, 800 m north along the road from Chilling, immediately before its tectonic boundary with the Upper Chilling Formation. A very distinctive outcrop of ophiolitic mélange outcrops on the hillside 2–3 km to the NW of Chilling (Fig. 16d). Here the ophiolitic mélange appears to sit directly above the Chilling Formation. Clift et al. (2001, 2002) consider this contact to be stratigraphic. The lack of ophiolite-

related detritus in the Chilling Formation (see Sections 5.2.2 and 5.2.3), might be considered unusual if the Chilling Formation were to be unconformably overlying the ophiolite mélange. However, the direct contacts between these formations are masked by scree slopes, disallowing for the precise nature of this contact to be determined, and therefore such a contact cannot be ruled out. A field photograph showing an overview of the relationships of the units mapped around Chilling is presented in Fig. 16d.

5.2. Compositional characterization of the Chilling Formation

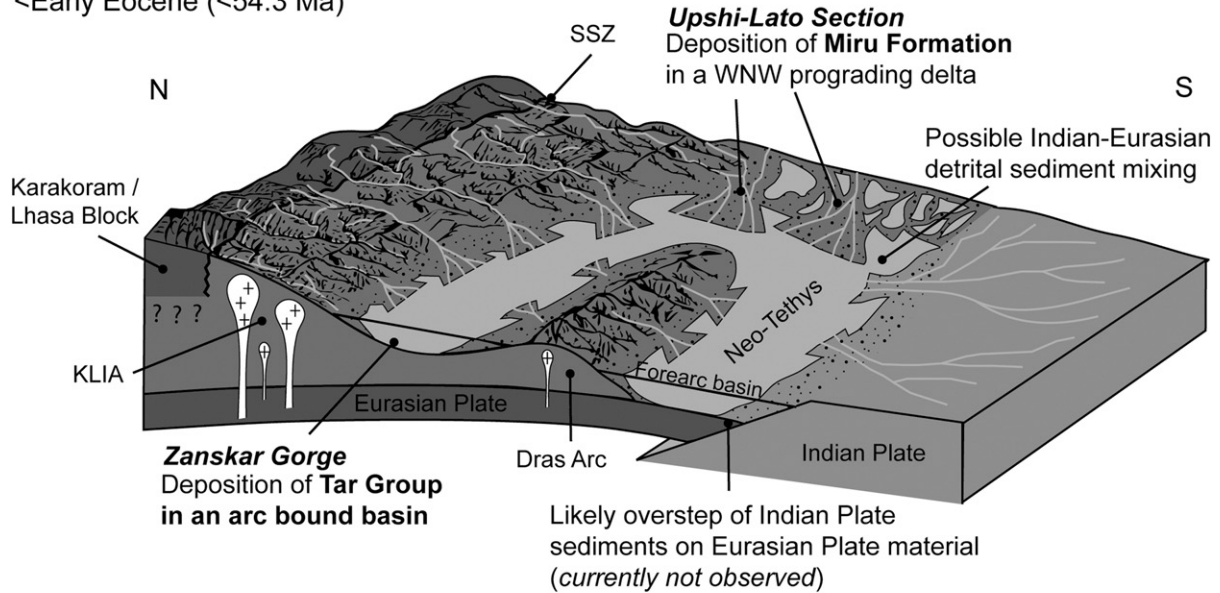
5.2.1. Mudstone geochemistry

As described in Section 4.2.1, Henderson et al. (2010b) and Garzanti and Van Haver (1988) showed that the youngest IBSR formations (e.g. the Choksti Formation) show enrichment in Cr and Ni relative to PAAS, whilst older rocks belonging to the Tar Group and Lower Indus Group are depleted relative to PAAS (Fig. 8). Three samples from the Chilling Formation were analyzed using the method outlined in Section 4.2.1. Results presented in Fig. 8 (and Section S1 of the Supplementary data) show that similar to the Indian-derived Lato Formation in the Upshi–Lato section (Section 4.2.1), Chilling Formation samples are more enriched in Cr and Ni compared to any IBSR or Lamayuru Indian plate sample (Fig. 8). Data from the Chilling ophiolitic mélange (published in Henderson et al. (2010b)) is also reproduced here.

5.2.2. Sandstone petrography

As described in Section 4.2.2, there is a gradual evolution in petrography from undissected to dissected arc provenance within the IBSR formations through time (Fig. 9). Two Chilling Formation sandstone samples were analyzed, using the methodology described in Section 4.2.2, with full results available in Section S2 of the Supplementary data. The petrography of the Chilling Formation samples is notably different to those from IBSR rocks, but similar to those of the Lato Formation in the Upshi–Lato section, plotting in the Recycled Orogen field (Fig. 9). These samples have an absence or very low abundance of feldspars, and lithic clasts are dominantly of sedimentary type. Chert and carbonate clasts occur in greater abundance than in the

a) Demise of Neo-Tethys in this region
<Early Eocene (<54.3 Ma)



b) Paleo-Indus River initiation in this region
Late Oligocene–Early Miocene

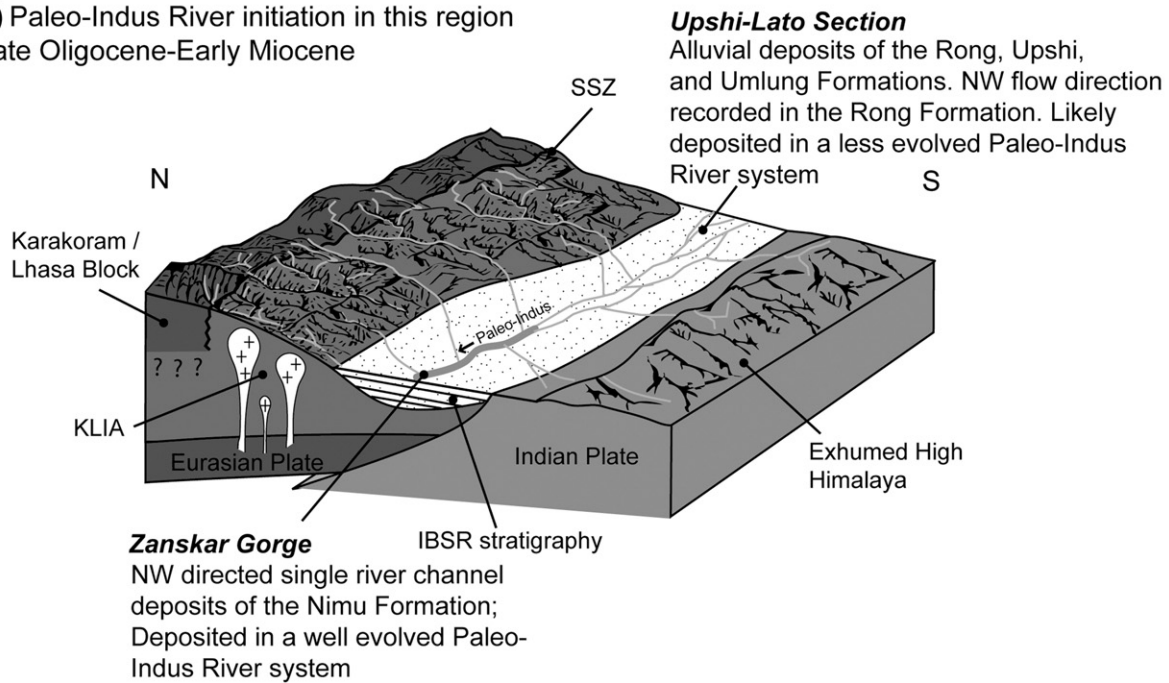


Fig. 14. A cartoon model of paleodepositional environments within the Indus Basin during (a) the deposition of the Miru Formation during Early-Eocene times at the demise of Neo-Tethys, and (b) the deposition of upper Indus Group formations during Late-Oligocene–Early Miocene times with initiation of the Paleo-Indus River system in this region at this time. Note that models are simplified and are not to scale.

IBSR samples, and grains of serpentinite and peridotite are not apparent. In contrast to the Lato Formation, detrital white micas, metamorphic psammites, and volcanic lithic clasts are absent.

5.2.3. Conglomerate clast counts

As shown in Fig. 10, breccias and conglomerates from the Chilling Formations are dominant in sedimentary lithic, chert, and quartzose clasts, similar to the conglomerates of the Lato Formation in the Lato–Upshi section (Section 4.2.3). Also present are limestone and quartzite

clasts. However, a very minor amount of granitoid and basalt clasts occur in the Lato Formation, but are absent in the Chilling Formation.

5.2.4. U–Pb ages of detrital zircons

Detrital zircons from an Upper Chilling Formation sample (ZG07030) were analyzed using the methodology as given in Section 4.2.4. Full data tables are presented in Section S3b of the Supplementary data, with the data presented alongside a compilation of zircon ages from both Indian and Eurasian plate sources displayed in Fig. 11. In contrast to IBSR

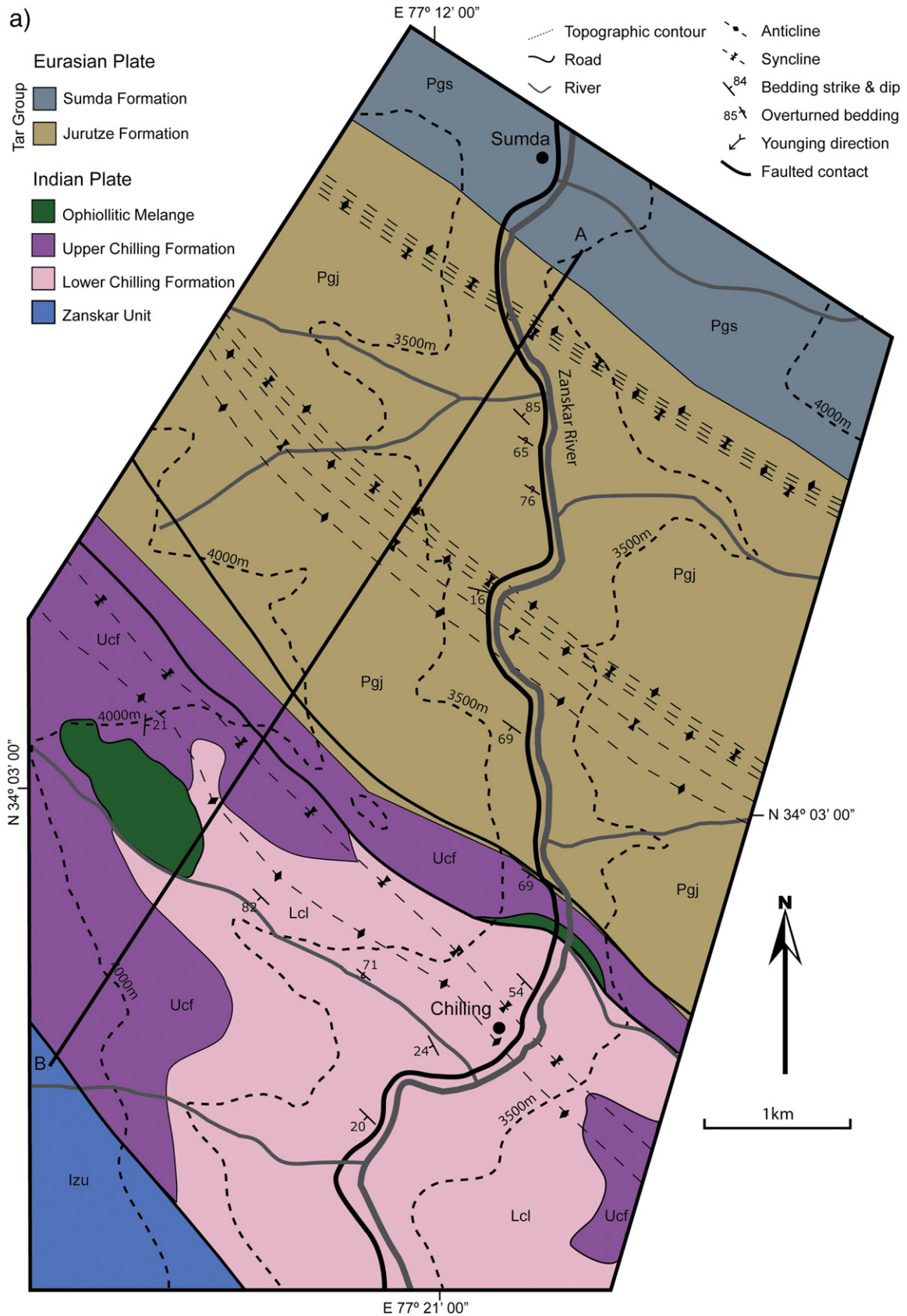


Fig. 15. (a) Geological map constructed during the field season in 2008 between the villages of Chilling and Sumda in the Zanskar Gorge, Ladakh (Field Area 2, section 5). Topographic contours are displayed in 500 m intervals taken from Pointet (2004). (b) Geological cross section between points A and B as displayed on the geological map in panel a. Younging direction arrows are provided for each formation. Key for Fig. 15: Izu – Zanskar Unit; Lcl – Lower Chilling Fm; Ucl – Upper Chilling Fm; Pgj – Jurutze Fm Pgs–Sumda Fm.

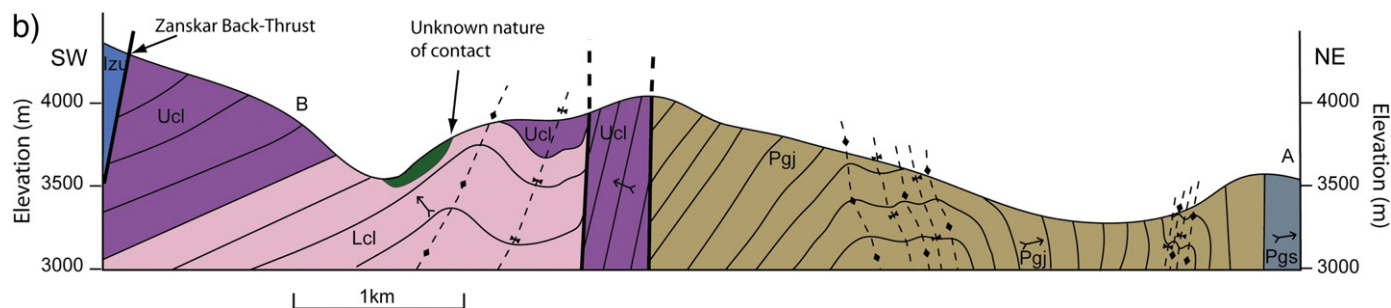


Fig. 15 (continued).

Table 3
Sedimentology of Formations described in Section 5, Field area 2, Chilling–Sumda area, Zanskar Gorge Section.

Lithologies	Sedimentology	Sedimentary structures
<p><i>Jurutze</i> Black shales and siltstones, gray phyllites. Fine grained dark ssts and carbonates present in upper part.</p>		
<p><i>Chilling Fm</i> Lower Chilling Black-gray slaty shales, blue phyllites, black crystalline limestone. Upper part of sequence consists of msts and shales, fine to coarse sst, breccias and congl with colors of red, green, black, gray, yellow, and purple.</p>	<p>Overall, upward coarsening sequence, but both upward coarsening and upward fining seen on local scale. Mudstones and ssts are usually well laminated. Black shales are organic rich and associated with Fe enrichment. Ssts are poorly cemented with a high proportion of muddy matrix. Congls, <10 m thick, are both clast and matrix supported, and often interbedded with thin subordinate well laminated lithic arenites, phyllites or shale. Breccia beds are 4 cm–1 m thick. Limestone clasts are present in breccia and congl.</p>	<p>Groove marks, sole casts, planar x-bedding and laminations, flaser bedding, ripple lamination, asymmetrical ripples, erosive bases, slumping, bioturbation, Fe nodules.</p>
<p>Upper Chilling Dominance of red/purple lithologies: well cleaved msts, fine to coarse silty-lithic arenites, breccias and pebble congl in purple sand matrix. Paleosols.</p>	<p>Congl and ssts <10–30 cm thick. Shales often >1 m thick. Pebble congl clasts held in poorly cemented fine grained purple sand matrix. No grading between beds, changes in grain size depicted by planar bedding or erosive bases.</p>	<p>Finer units are well laminated. Ssts preserve faint planar x-beds, bioturbation, dewatering structures. Slumping in coarser units.</p>
<p><i>Chilling ophiolitic melange</i> Dark green breccias, conglomerates and ssts.</p>	<p>Congl with ophiolitic clast lithologies e.g. chert, gabbro, serpentinite. Angular to subangular ssts interbed the conglomerates.</p>	<p>Ssts often have normal grading, erosive bases and rip-up clasts.</p>

samples but similar to the Lato Formation samples, the Upper Chilling Formation sample is dominated by older Paleozoic and Precambrian aged assemblages, with only a rare, subordinate proportion of younger grains; the youngest dated at 159.2 (\pm 4.0) Ma.

5.3. Provenance of the Chilling Formation

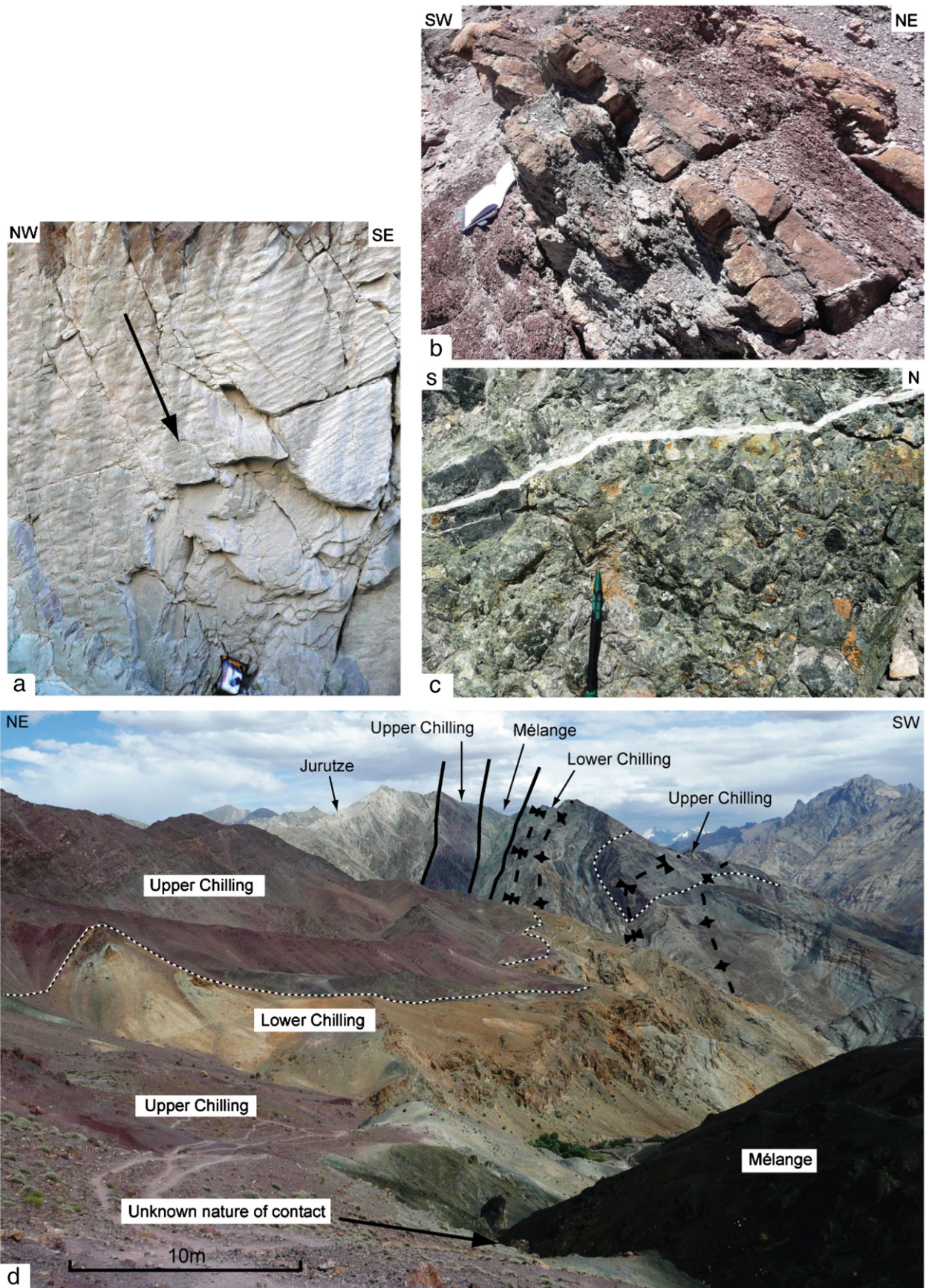
Sandstone petrography shows that detrital material in Chilling Formation sandstone samples were derived from a Recycled Orogen provenance (Fig. 9; as defined by Dickinson and Suczek, 1979). This, plus the lack of granitoid conglomerate clasts, and the dominance of Paleozoic to Precambrian U–Pb zircon ages with accompanying lack of Cretaceous–Paleogene U–Pb ages, indicates dominant sediment derivation from the Indian rather than Asian plate. A source area with an exact match in grain ages for the single 159.2 (\pm 4.0) Ma aged zircon grain has not been found. It may have been derived from an ophiolite

assemblage of rocks of Triassic–Cretaceous age obducted onto the Indian Margin. Zircons dated at 177 Ma and 88 Ma have been documented from the Spontang ophiolite (Pedersen et al., 2001). Although there is a lack of ophiolitic clasts in the formation, the high Cr and Ni concentrations, approaching values for the ophiolitic mélange (Fig. 8) indicates ophiolitic input. A possible reason for the discrepancy between mudstone geochemistry and clast lithologies could be that ophiolitic material originated from a more distal source and is therefore only preserved in the sub-sand grade detritus, whereas sedimentary material was likely sourced from a more proximal region, therefore forming the dominant sandstone and conglomerate clast composition frameworks.

5.4. Correlation of the Chilling Formation

Our defined Chilling Formation has been assigned to a variety of geological formations by several different authors. Fuchs (1986)

Fig. 16. Field photos (Chilling–Sumda area, Field area 2). (a) Asymmetrical ripples within fine gray sandstones in the Lower Chilling Formation. Flow is indicated by the arrow. N 34° 02' 43.9" E 077° 11' 32.2". (b) Brown sandstone and red shale beds of the Upper Chilling Formation. Taken from N 34° 03' 34.6" E 077° 10' 52.8". (c) Chilling ophiolitic mélange breccia. Clasts of ultramafic igneous, basalt, chert, and serpentinite held within a green sand matrix. Taken from N 34° 02' 41.7" E 077° 12' 43.4". (d) Field photograph looking SE displaying field relations observed near to the village of Chilling. Thick black lines indicate faults. Mélange refers to the ophiolitic mélange breccia (see panel c). Black–white dashed line indicates conformable contact between the Lower and Upper Chilling Formations. (For interpretation of the references to color in this figure legend, the reader is referred to the



assigned the red-green colored clastic succession surrounding Chilling to represent the youngest section of the volcanoclastic sediments of the Dras unit (described in Fuchs, 1981), also naming it the “Chilling Formation”. Brookfield and Andrews-Speed (1984) could not correlate this unit and referred to it as “unassigned molasse”. Searle et al. (1990) considered this unit to represent both Chogdo and Nindam lithologies, whereas Clift et al. (2001, 2002) assigned this same unit to both Chogdo and Khalsi Limestone formations.

We do not agree that the rocks that we term the Chilling Formation can be correlated with the Chogdo Formation of the Zaskar Gorge “type section” as defined in Henderson et al. (2010b) (Fig. 2). The reasoning for this is the geochemical characteristics of the rocks are radically different to Chogdo Formation signatures: the detrital zircon assemblage in the Chilling Formation consists of old, most probably Indian derived grains (Fig. 11), with the absence of a dominant young arc-derived age assemblage which is a key characteristic of Chogdo and other IBSR formations (Wu et al., 2007; Henderson et al., 2010b). Sandstone petrographic composition plots in the Recycled Orogenic field (Fig. 9) and conglomerate clasts are dominantly sedimentary derived (Fig. 10). This contrasts with IBSR rocks where sandstones plot in the transitional-dissected arc field and conglomerate clasts are dominated by plutonic, volcanic and ultramafic igneous clasts (Henderson et al., 2010b). Mudstone geochemistry shows significant enrichment in Cr and Ni, concentrations, more so than any analyzed Indus Basin sedimentary rock (Garzanti and van Haver, 1988; Fig. 8; Henderson et al., 2010b). Finally, facies of the Upper Chilling Formation are distinct from those of the Chogdo Formation; the presence of interbedded red colored erosive conglomerates, sandstone beds and lenses, and bioturbated mudstones with associated paleosols in the Upper Chilling Formation (Table 3) are not present in the Chogdo Formation (Henderson et al., 2010b), and, unlike the Chogdo Formation, interbedded limestones are absent. In conclusion, we do not consider these rocks to be Chogdo Formation, and we do not endorse correlation between this unit, which we term the Chilling Formation, with the Chogdo Formation of the Zaskar Gorge, with which it has previously been correlated.

We tentatively speculate a possible correlation between the lower Chilling Formation and the Lamayuru Formation. The Lamayuru Formation has been mapped by several authors (as mentioned above), again somewhat inconsistently in this area. Although not considered a separate formation in this mapping project, we suggest that the fine grained facies of carbonates, black shales, and phyllites in the lower stratigraphic levels of the Lower Chilling formation (Section 5.1.2), could be correlative with the Lamayuru Formation representing marine sedimentation on the Indian Passive margin. However, we recognize that the mudstone geochemistry is different between these two units.

Results from our study reveal that compositional similarities exist between the Chilling Formation and the Lato Formation, with both formations having a dominant sediment derivation from the Indian Plate. Combining this with their similar along-strike position makes the correlation between these two formations a possibility, worthy of further investigation. Subtle differences in compositional nature (e.g. the presence of detrital micas and granitoid clasts in the Lato Formation, absent in the Chilling Formation) may reflect local drainage differences from specific restricted catchment areas.

5.5. Examining evidence for India–Eurasia collision at the Chilling–Sumda section

Using the data presented above, we now assess the validity of the two stratigraphic contacts in this area outlined by Clift et al. (2001, 2002) which are suggested to show evidence of India–Eurasia collision (Table 2). Distinctively colored red clastic rocks outcropping around the Chilling area were considered by Clift et al. (2001, 2002) to be the Asian-derived Chogdo Formation. This interpretation was

based on facies and palaeoflow indicators that these authors considered were similar to those of the defined Chogdo Formation further north in the Zaskar Gorge. Clift et al. (2001, 2002) interpreted their identified Chogdo Formation to unconformably overlie both the Indian Plate Lamayuru Formation and ophiolitic mélangé, both thought to be of Indian Plate affinity. Such a scenario, if correct, would constrain the time of collision at 50.8–51 Ma, this age being the depositional age of the Eurasian-derived Chogdo Formation, as determined in the type section to the north in the Zaskar Gorge.

However, our data indicate that the red clastic formation outcropping around the village of Chilling, (which we have named the Upper Chilling Formation) cannot be correlated with the IBSR Chogdo Formation, contrary to the proposals of Searle et al. (1990) and Clift et al. (2001, 2002), as discussed in Section 5.4. Instead, the data indicate that these rocks are Indian-derived (Section 5.3), and therefore cannot be used to constrain the time of arrival of Eurasian detritus onto the Indian plate. Therefore, the Eurasian–Indian stratigraphic contacts proposed by Clift et al. (2001, 2002) for constraining the timing of India–Eurasia collision are now considered untenable for this purpose due to the clear Indian provenance of the Chilling Formation and its now invalid correlation to the Chogdo Formation. In summary, the geology surrounding the village of Chilling does not show any valid stratigraphic relationships of Eurasian plate material overlying Indian plate rocks (Table 2).

6. Summary and conclusions

In the Indus–Tsangpo suture zone, at key locations in the Zaskar Gorge and along the Manali–Leh Highway, previous work has interpreted Asian-derived 50.8–51 Ma Chogdo Formation to stratigraphically overlie Indian plate sequences, thus constraining India–Asia collision to have occurred by this time. We challenge this view. Our petrographic, geochemical, isotopic and facies examination of the geology at these key localities exposed both along the Upshi–Lato transect on the Manali–Leh Highway, and also surrounding the village of Chilling in the Zaskar Gorge, Ladakh has refuted the interpretation that the Eurasian derived 50.8–51 Ma Chogdo Formation stratigraphically overlies Indian plate rocks in the locations described in previous publications. At the critical locations, we argue that rocks previously assigned to the Chogdo Formation and/or Indian plate have been incorrectly identified and/or correlated. Such stratigraphic relationships can therefore not be used to constrain the time of collision as previously proposed. In addition to stratigraphic evidence, the Chogdo Formation has also previously been proposed to show earliest evidence of mixed Indian–Asian detritus (Clift et al., 2001, 2002), thus providing an alternative approach to constraining the time of collision using the IBSR. We also disagree with this premise, as discussed in Henderson et al. (2010b) in which we argue that there is no unequivocal evidence for Indian derived input into the IBSR until higher up in the succession. Thus, careful scrutiny of the utility of the IBSR to constrain collision in previous research needs to be applied. Furthermore, if the recent concept that the Kohistan–Ladakh island arc may have collided with India before Asia is upheld (Bouilhol et al., 2010), then interpretations based on all previous sedimentological work constraining the time of India–Asia collision based on the appearance of an “Asian” detrital signature on the Indian plate needs to be reevaluated.

Our paleoenvironmental interpretation of IBSR exposure along the Upshi–Lato transect proposes that during the demise of the Neo-Tethys Ocean, a NW prograding delta developed into the closing seaway at no earlier than Early Eocene times. An unconformity likely represents a gap in depositional history from ~Mid Eocene to Early Oligocene times when the sedimentation record is resumed, with the Mid to Upper Indus Group formations. These Indus Group sediments may have been deposited in a NW flowing fluvial system, representing an early stage Paleo-Indus River system. Sedimentation of the IBSR

within the Indus Tsangpo Suture Zone continued until at least Early Miocene times.

Supplementary materials related to this article can be found online at doi:10.1016/j.earscirev.2011.02.006.

Acknowledgements

This work was funded by NERC grant NE/D000092/1 to YN, NERC PhD studentship NER/S/A/2006/14020 to ALH, and NIGL Facilities grants for U–Pb and Ar–Ar analyses. Thanks are due to NIGL, Keyworth, for help with sample preparation and U–Pb analysis. NERC is thanked for continued funding of the Argon Isotope Facility and SUERC is funded by the Scottish Universities. Jennifer Smith and Abigail Adams (University of Glasgow) are thanked for assistance with sample preparation as a part of the AIF Summer Internship. Dan Barford (SUERC) is thanked for analysis of two $^{40}\text{Ar}/^{39}\text{Ar}$ samples, Fida Hussein for help with field logistics and Alistair Bargery, Tom Webster and Mike Gallagher for field assistance. We also thank Mike Searle and Rick Law for their insightful discussions in the field.

References

- Ahmad, T., et al., 2000. Isotopic constraints on the structural relationships between the Lesser Himalayan Series and the High Himalayan Crystalline Series, Garhwal Himalaya. *Geological Society of America Bulletin* 112 (3), 467–477.
- Aitchison, J.C., Ali, J.R., Davis, A.M., 2007. When and where did India and Asia collide? *Journal of Geophysical Research* 112. doi:10.1029/2006JB004706.
- Allegre, C.J., Othman, D.B., 1980. Nd–Sr isotopic relationship in granitoid rocks and continental crust development: a chemical approach to orogenesis. *Nature* 286 (5771), 335–342.
- Ayres, M.W., 1997. Trace-Element Behaviour during High-grade Metamorphism and Anatexis of the Himalayas. Open University.
- Baud, A., Arn, R., Bugnon, P., Crisnel, A., Dolivo, E., Escher, A., Hammerschlag, J.-G., Marthaler, M., Masson, H., Steck, A., Tieche, J.-C., 1982. Le contact Gondwana – peri-Gondwana dans le Zaskar oriental (Ladakh, Himalaya). *Bulletin. Société Géologique de France* 24 (2), 341–361.
- Bouilhol, P., Jagoutz, O., Hanchar, J.M., 2010. The change of source composition in plutonic rocks from the Kohistan–Ladakh arc constrain the onset of collision along the Indus Suture in the western Himalaya. *Geological Society of America Abstracts with Programs* 42 (5), 664 Paper 285–3.
- Brookfield, M.E., Andrews-Speed, C.P., 1984. Sedimentology, petrography and tectonic significance of the shelf, flysch and molasse clastic deposits across the Indus Suture Zone, Ladakh, NW India. *Sedimentary Geology* 40 (4), 249–286.
- Chu, M.-F., et al., 2006. Zircon U–Pb and Hf isotope constraints on the Mesozoic tectonics and crustal evolution of southern Tibet. *Geology* 34, 745–748.
- Chung, S.-L., et al., 2005. Tibetan tectonic evolution inferred from spatial and temporal variations in post-collisional magmatism. *Earth-Science Reviews* 68 (3–4), 173–196.
- Clift, P.D., Degnan, P.J., Hannigan, R., Blusztajn, J., 2000. Sedimentary and geochemical evolution of the Dras forearc basin, Indus suture, Ladakh Himalaya, India. *Geological Society of America Bulletin* 112 (3), 450–466.
- Clift, P.D., Shimizu, N., Layne, G.D., Blusztajn, J., 2001. Tracing patterns of erosion and drainage in the Paleogene Himalaya through ion probe Pb isotope analysis of detrital K-feldspars in the Indus Molasse, India. *Earth and Planetary Science Letters* 188 (3–4), 475–491.
- Clift, P.D., Carter, A., Krol, M., Kirby, E., 2002. Constraints on India–Eurasia collision in the Arabian sea region taken from the Indus Group, Ladakh Himalaya, India. The tectonic and climatic evolution of the Arabian Sea region. *Geological Society of London Special Publication* 195, 97–116.
- Corfield, R.I., Searle, M.P., Green, O.R., 1999. Photang thrust sheet: an accretionary complex structurally below the Spontang ophiolite constraining timing and tectonic environment of ophiolite obduction, Ladakh Himalaya, NW India. *Journal of the Geological Society* 156 (5), 1031–1044.
- de Sigoyer, J., et al., 2000. Dating the Indian continental subduction and collisional thickening in the northwest Himalaya: multichronology of the Tso Moriri eclogites. *Geology* 28 (6), 487–490.
- Debon, F., Le Fort, P., Sheppard, S.M.F., Sonet, J., 1986. The four plutonic belts of the Trans-Himalaya–Himalaya: a chemical, mineralogical, isotopic and chronological synthesis along a Tibet–Nepal section. *Journal of Petrology* 27, 219–250.
- Deniel, C., Vidal, P., Fernandez, A., Le Fort, P., Peucat, J.J., 1987. Isotopic study of the Manaslu granite (Himalaya, Nepal): inferences on the age and source of Himalayan leucogranites. *Contributions to Mineralogy and Petrology* 96, 78–92.
- Dickinson, W.R., 1985. Interpreting provenance relations from detrital modes of sandstones. In: Zuffa, G.G. (Ed.), *Provenance of Arenites*. NATO ASI, Reidel, Dordrecht, pp. 333–361.
- Dickinson, W.R., Suzeck, C.A., 1979. Plate tectonics and sandstone compositions. *American Association of Petroleum Geologists Bulletin* 63 (12), 2164–2182.
- Ding, L., Kapp, P., Wan, X.Q., 2005. Paleocene–Eocene record of ophiolite obduction and initial India–Asia collision, south central Tibet. *Tectonics* 24 (3), TC3001.
- Foster, G., Carter, A., 2007. Insights into the patterns and locations of erosion in the Himalaya – a combined fission track and in situ Sm–Nd isotopic study of detrital apatite. *Earth and Planetary Science Letters* 257, 407–418.
- Foster, G.L., Vance, D., 2006. In situ Nd isotopic analysis of geological materials by laser ablation MC–ICP–MS. *Journal of Analytical Atomic Spectrometry* 21, 288–296.
- Foster, G., Kinny, P., Vance, D., Prince, C., Harris, N., 2000. The significance of monazite U–Th–Pb age data in metamorphic assemblages; a combined study of monazite and garnet chronometry. *Earth and Planetary Science Letters* 181, 327–340.
- France-Lanord, C., Derry, L., Michard, A., 1993. Evolution of the Himalaya since Miocene time: isotopic and sedimentological evidence from the Bengal Fan. In: Treloar, P.J., Searle, M.P. (Eds.), *Himalayan Tectonics*. Geological Society Special Publication, pp. 603–622.
- Fuchs, G., 1981. Outline of the geology of the Himalaya. *Mitteilungen der Oesterreichischen Geologischen Gesellschaft* 74, 101–127.
- Fuchs, G., 1986. The geology of the Markha–Khurnak region in Ladakh (India). *Jahrbuch Geologischer Bundesanstalt-A* 128 (3–4), 403–437.
- Fuchs, G., Linner, M., 1995. Geological traverse across the western Himalaya: a contribution to the geology of eastern Ladakh, Lahul and Chamba. *Jahrbuch Geologischer Bundesanstalt-A* 138, 655–685.
- Fuchs, G., Linner, M., 1996. On the geology of the suture zone and Tso Moriri Dome in Eastern Ladakh (Himalaya). *Jahrbuch Geologischer Bundesanstalt-A* 139, 191–207.
- Gaetani, M., Garzanti, E., 1991. Multicyclic history of the Northern India Continental-Margin (Northwestern Himalaya). *American Association of Petroleum Geologists Bulletin* 75 (9), 1427–1446.
- Garzanti, E., van Haver, T., 1988. The Indus clastics – fore-arc basin sedimentation in the Ladakh Himalaya (India). *Sedimentary Geology* 59 (3–4), 237–249.
- Garzanti, E., Baud, A., Mascle, G., 1987. Sedimentary record of the Northward Flight of India and its collision with Eurasia (Ladakh Himalaya, India). *Geodinamica Acta* 1 (4–5), 297–312.
- Gehrels, G.E., et al., 2003. Initiation of the Himalayan orogen as an Early Paleozoic thin-skinned thrust belt. *GSA Today* 13 (9), 4–9.
- Green, O.R., Searle, M.P., Corfield, R.I., Corfield, R.M., 2008. Cretaceous–Tertiary carbonate platform evolution and the age of the India–Asia collision along the Ladakh Himalaya (Northwest India). *The Journal of Geology* 116 (4), 331–353.
- Harrison, T.M., et al., 2000. The Zedong window: a record of superposed Tertiary convergence in southeastern Tibet. *Journal of Geophysical Research* 105, 19211–19230.
- Henderson, A.L., Foster, G.L., Najman, Y., 2010a. Testing the application of in situ Sm–Nd isotopic analysis on detrital apatites: a provenance tool for constraining the timing of India–Eurasia collision. *Earth and Planetary Science Letters* 297 (1–2), 42–49.
- Henderson, A.L., et al., 2010b. The geology of the Cenozoic Indus Basin sedimentary rocks; palaeoenvironmental interpretation of sedimentation from the western Himalaya during the early phases of India–Eurasia collision. *Tectonics* 29.
- Honegger, K., Le Fort, P., Mascle, G., Zimmermann, J.-L., 1989. The blueschists along the Indus Suture Zone in Ladakh, NW Himalaya. *Journal of Metamorphic Geology* 7 (1), 57–72.
- Inger, S., Harris, N., 1993. Geochemical constraints on leucogranite magmatism in the Langtang Valley, Nepal Himalaya. *Journal of Petrology* 34 (2), 345–368.
- Ingersoll, R.V., et al., 1984. The effect of grain-size on detrital modes: a test of the Gazi–Dickinson point-counting method. *Journal of Sedimentary Petrology* 54, 103–116.
- Jacobsen, S.B., Wasserburg, G.J., 1980. Sm–Nd isotopic evolution of chondrites. *Earth and Planetary Science Letters* 50 (1), 139–155.
- Jaeger, J.J., Courtillot, V., Tapponnier, P., 1989. Paleontological view of the ages of the Deccan Traps, the Cretaceous Tertiary Boundary, and the India–Asia collision. *Geology* 17 (4), 316–319.
- Jagoutz, O., Müntener, O., Burg, J.P., Ulmer, P., Jagoutz, E., 2006. Lower continental crust formation through focused flow in km-scale melt conduits: the zoned ultramafic bodies of the Chilas Complex in the Kohistan Island arc (NW Pakistan). *Earth and Planetary Science Letters* 242 (3–4), 320–342.
- Khan, M.A., Stern, R.J., Gribble, R.F., Windley, B.F., 1997. Geochemical and isotopic constraints on subduction polarity, magma sources, and palaeogeography of the Kohistan intra-oceanic arc, northern Pakistan Himalaya. *Journal of the Geological Society* 154 (6), 935–946.
- Klootwijk, C.T., Gee, J.S., Peirce, J.W., Smith, G.M., McFadden, P.L., 1992. An early India–Asia contact – paleomagnetic constraints from Ninetyeast Ridge, ODP Leg 121. *Geology* 20 (5), 395–398.
- Leech, M.L., Singh, S., Jain, A.K., Klemperer, S.L., Manickavasagam, R.M., 2005. The onset of India–Asia continental collision: early, steep subduction required by the timing of UHP metamorphism in the western Himalaya. *Earth and Planetary Science Letters* 234 (1–2), 83–97.
- Leier, A.L., DeCelles, P.G., Kapp, P., Ding, L., 2007. The Takena Formation of the Lhasa terrane, southern Tibet: the record of a Late Cretaceous retroarc foreland basin. *Geological Society of America Bulletin* 119 (1–2), 31–48.
- Ludwig, K.R., 2003. *Isoplot*.
- Mahéo, G., et al., 2004. The South Ladakh ophiolites (NW Himalaya, India): an intra-oceanic tholeiitic arc origin with implication for the closure of the Neo-Tethys. *Chemical Geology* 203 (3–4), 273–303.
- Mark, D.F., Barford, D., Stuart, F.M., Imlach, J., 2009. The ARGUS multicollector noble gas mass spectrometer: performance for $^{40}\text{Ar}/^{39}\text{Ar}$ geochronology. *Geochem. Geophys. Geosyst.* 10.
- McElroy, R., Cater, J., Roberts, I., Peckham, A., Bond, M., 1990. The structure and stratigraphy of SE Zaskar, Ladakh Himalaya. *Journal of the Geological Society* 147 (6), 989–997.
- Miller, C., Klotzli, U., Frank, W., Thoni, M., Grasemann, B., 2000. Proterozoic crustal evolution in the NW Himalaya (India) as recorded by circa 1.80 Ga mafic and 1.84 Ga granitic magmatism. *Precambrian Research* 103, 191–206.

- Miller, C., et al., 2001. The early Palaeozoic magmatic event in the Northwest Himalaya, India: source, tectonic setting and age of emplacement. *Geological Magazine* 138, 237–251.
- Molnar, P., Tappanier, P., 1975. Cenozoic tectonics of Asia — effects of a continental collision. *Science* 189 (4201), 419–426.
- Murphy, M.A., et al., 1997. Significant crustal shortening in south-central Tibet prior to the Indo-Asia collision. *Geology* 25, 719–722.
- Oliver, G.J.H., Johnson, M.R.W., Fallick, A.E., 1995. Age of metamorphism in the Lesser Himalaya and the Main Central Thrust Zone, Garhwal India — results of illite crystallinity, Ar-40–Ar-39 fusion and K–Ar studies. *Geological Magazine* 132 (2), 139–149.
- Parrish, R.R., Hodges, K.V., 1996. Isotopic constraints on the age and provenance of the Lesser and Greater Himalayan sequences, Nepalese Himalaya. *Geological Society of America Bulletin* 108 (7), 904–911.
- Parrish, R.R., Gough, S.J., Searle, M.P., Waters, D.J., 2006. Plate velocity exhumation of ultrahigh-pressure eclogites in the Pakistan Himalaya. *Geology* 34 (11), 989–992.
- Patriat, P., Achache, J., 1984. India Eurasia collision chronology has implications for crustal shortening and driving mechanism of plates. *Nature* 311 (5987), 615–621.
- Pedersen, R.B., Searle, M.P., Corfield, R.I., 2001. U–Pb zircon ages from the Spontang Ophiolite, Ladakh Himalaya. *Journal of the Geological Society* 158 (3), 513–520.
- Petterson, M.G., Crawford, M.B., Windley, B.F., 1993. Petrogenetic implications of neodymium isotope data from the Kohistan batholith, North Pakistan. *Journal of the Geological Society* 150 (1), 125–129.
- Pointet, A., 2004. Ladakh and Zaskar Centre: Indus–Zaskar–Pangong, India: Ed. Olizane Trekking Maps of Ladakh and Zaskar. Editions Olizane.
- Powell, C.M., Conaghan, P.J., 1973. Plate tectonics and the Himalayas. *Earth and Planetary Science Letters* 20, 1–12.
- Prince, C.I., 1999. The Timing of Prograde Metamorphism in the Garhwal Himalaya, India. The Open University.
- Rage, J.C., et al., 1995. Collision age. *Nature* 375 (6529), 286.
- Ramsey, M.H., et al., 1995. An objective assessment of analytical method precision: comparison of ICP-AES and XRF for the analysis of silicate rocks. *Chemical Geology* 124 (1–2), 1–19.
- Raymo, M.E., Ruddiman, W.F., 1992. Tectonic forcing of Late Cenozoic climate. *Nature* 359 (6391), 117–122.
- Reuber, I., 1989. The Dras arc — 2 successive volcanic events on eroded oceanic-crust. *Tectonophysics* 161 (1–2), 93–106.
- Richter, F.M., Rowley, D.B., Depaolo, D.J., 1992. Sr isotope evolution of seawater — the role of tectonics. *Earth and Planetary Science Letters* 109 (1–2), 11–23.
- Robertson, A., 1998. Rift-related sedimentation and volcanism of the north-Indian margin inferred from a Permian–Triassic exotic block at Lamayuru, Indus suture zone (Ladakh Himalaya) and regional comparisons. *Journal of Asian Earth Sciences* 16 (2–3), 159–172.
- Robertson, A.H.F., 2000. Formation of melanges in the Indus Suture Zone, Ladakh Himalaya by successive subduction-related, collisional and post-collisional processes during Late Mesozoic–Late Tertiary time. *Geological Society of London. Special Publication* 170 (1), 333–374.
- Robertson, A.H.F., Degnan, P.J., 1993. Sedimentology and tectonic implications of the Lamayuru Complex: deep water facies of the Indian Passive margin. In: Searle, M.P., Treloar, P.J. (Eds.), *Himalayan Tectonics*. Geological Society of London Special Publication, pp. 299–322.
- Robertson, A., Degnan, P., 1994. The Dras arc complex — lithofacies and reconstruction of a Late Cretaceous oceanic volcanic arc in the Indus Suture Zone, Ladakh–Himalaya. *Sedimentary Geology* 92 (1–2), 117–145.
- Rowley, D.B., 1996. Age of initiation of collision between India and Asia: a review of stratigraphic data. *Earth and Planetary Science Letters* 145 (1–4), 1–13.
- Schärer, U., Xu, R.-H., Allègre, C.J., 1984. UPb geochronology of Gangdese (Trans-Himalaya) plutonism in the Lhasa–Xigaze region, Tibet. *Earth and Planetary Science Letters* 69 (2), 311–320.
- Schärer, U., Copeland, P., Harrison, T.M., Searle, M.P., 1990. Age, cooling history, and origin of post-collisional leucogranites in the Karakoram Batholith: a multi-system isotope study. *Journal of Geology* 98 (2), 233–251.
- Schlup, M., Carter, A., Cosca, M., Steck, A., 2003. Exhumation history of eastern Ladakh revealed by Ar–Ar and fission-track ages: the Indus River–Tso Moriri transect, NW Himalaya. *Journal of the Geological Society, London* 160, 385–399.
- Searle, M.P., et al., 1987. The closing of Tethys and the tectonics of the Himalaya. *Geological Society of America Bulletin* 98 (6), 678–701.
- Searle, M.P., Cooper, D.J.W., Rex, A.J., 1988. Collision tectonics of the Ladakh–Zaskar Himalaya. In: Shackleton, R.M., Dewey, J.F., Windley, B.F. (Eds.), *Tectonic Evolution of the Himalayas and Tibet*. Philosophical Transactions of the Royal Society of London, pp. 117–150.
- Searle, M.P., Pickering, K.T., Cooper, D.J.W., 1990. Restoration and evolution of the intermontane Indus Molasse Basin, Ladakh Himalaya, India. *Tectonophysics* 174 (3–4), 301–314.
- Searle, M.P., Waters, D.J., Rex, D.C., Wilson, R.N., 1992. Pressure, temperature and time constraints on Himalayan metamorphism from Eastern Kashmir and Western Zaskar. *Journal of the Geological Society* 149, 753–773.
- Searle, M., Corfield, R.I., Stephenson, B., McCarron, J., 1997. Structure of the North Indian continental margin in the Ladakh–Zaskar Himalayas: implications for the timing of obduction of the Spontang ophiolite, India–Asia collision and deformation events in the Himalaya. *Geological Magazine* 134 (3), 297–316.
- Simpson, R.L., Parrish, R.R., Searle, M.P., Waters, D.J., 2000. Two episodes of monazite crystallization during metamorphism and crustal melting in the Everest region of the Nepalese Himalaya. *Geology* 28 (5), 403–406.
- Sinclair, H.D., Jaffey, N., 2001. Sedimentology of the Indus Group, Ladakh, northern India: implications for the timing of initiation of the palaeo-Indus River. *Journal of the Geological Society* 158, 151–162.
- Steck, A., 2003. Geology of the NW Indian Himalaya. *Eclogae Geologicae Helveticae* 96 (2), 147–U13.
- Stutz, E., Thöni, M., 1987. The lower Paleozoic Nyimaling Granite in the Indian Himalaya (Ladakh): new Rb/Sr data versus zircon typology. *Geologische Rundschau* 76 (2), 307–315.
- Sutre E., 1990. Les formations de la marge nord-Neotethsienne et les melanges ophiolitiques de la zone de suture de l'Indus en Himalaya du Ladakh. PhD Thesis, L'Universite de Poitiers, 295 pp.
- Taylor, S.R., McLennan, S.M., 1985. The continental crust: its composition and evolution. An Examination of the Geochemical Record Preserved in Sedimentary Rocks. *Geoscience Texts*. Blackwell Scientific Publications.
- Tewari, V.C., 1993. Precambrian and Lower Cambrian stromatolites of the Lesser Himalaya. *Geophytology* 23, 19–39.
- Tonarini, S., et al., 1993. Eocene age of eclogite metamorphism in Pakistan Himalaya — implications for India Eurasia collision. *Terra Nova* 5 (1), 13–20.
- Treloar, P.J., et al., 1989. K–Ar and Ar–Ar geochronology of the Himalayan collision in Nw Pakistan — constraints on the timing of suturing, deformation, metamorphism and uplift. *Tectonics* 8 (4), 881–909.
- Treloar, P.J., Petterson, M.G., Jan, M.Q., Sullivan, M.A., 1996. A re-evaluation of the stratigraphy and evolution of the Kohistan arc sequence, Pakistan Himalaya: implications for magmatic and tectonic arc-building processes. *Journal of the Geological Society* 153 (5), 681–693.
- Valdiya, K.S., Bhatia, S.B. (Eds.), 1980. *Stratigraphy and Correlations of Lesser Himalayan Formations*. Hindustan Publishing Corporation, India. 330 pp.
- van Haver, T., 1984. Etude stratigraphique, sedimentologique et structurale d'un bassin d'avant arc: Exemple du bassin de l'Indus, Ladakh, Himalaya, Univ. de Grenoble, France, Grenoble. 204 pp.
- Vance, D., Harris, N., 1999. Timing of prograde metamorphism in the Zaskar Himalaya. *Geology* 27 (5), 395–398.
- Vannay, J.C., Hodges, K.V., 1996. Tectonometamorphic evolution of the Himalayan metamorphic core between Annapurna and Dhaulagiri, central Nepal. *Journal of Metamorphic Geology* 14 (5), 635–656.
- Walker, J.D., et al., 1999. Metamorphism, melting, and extension: age constraints from the High Himalayan Slab of southeast Zaskar and northwest Lahaul. *Journal of Geology* 107 (4), 473–495.
- Watson, J.S., 1996. Fast, simple method of powder pellet preparation for X-ray fluorescence analysis. *X-Ray Spectrometry* 25 (4), 173–174.
- Wen, D.-R., et al., 2008. Zircon SHRIMP U–Pb ages of the Gangdese Batholith and implications for Neotethyan subduction in southern Tibet. *Chemical Geology* 252 (3–4), 191–201.
- Whittington, A., Foster, G., Harris, N., Vance, D., Ayres, M., 1999. Lithostratigraphic correlations in the western Himalaya — an isotopic approach. *Geology* 27 (7), 585–588.
- Wu, F.Y., Clift, P.D., Yang, J.H., 2007. Zircon Hf isotopic constraints on the sources of the Indus Molasse, Ladakh Himalaya, India. *Tectonics* 26 (2).
- Xu, R.H., Schärer, U., Allègre, C.J., 1985. Magmatism and metamorphism in the Lhasa Block (Tibet): a geochronological study. *The Journal of Geology* 93 (1), 41–57.
- Yin, A., 2006. Cenozoic tectonic evolution of the Himalayan orogen as constrained by along-strike variation of structural geometry, exhumation history, and foreland sedimentation. *Earth-Science Reviews* 76 (1–2), 1–131.
- Yin, A., Harrison, T.M., 2000. Geological evolution of the Himalayan–Tibetan orogen. *Annual Reviews of Earth and Planetary Sciences* 28, 211–280.